Aus der Arbeitsgruppe Cellular Neurosciences des Max-Delbrück-Centrums für Molekulare Medizin in der Helmholtz-Gemeinschaft und dem Aflac Cancer and Blood Disorders Center der Emory University

DISSERTATION

Subtype-specific differences in the cellular glioblastoma microenvironment

zur Erlangung des akademischen Grades
Doctor medicinae (Dr. med.)

vorgelegt der Medizinischen Fakultät
Charité – Universitätsmedizin Berlin

von

Ioannis Kaffes

aus Larisa

Datum der Promotion: 25.11.2022

Table of Contents

List of Abbreviations **3**

Abstract **4**

Synopsis **8**

Introduction **8**

Methods **11**

The Cancer Genome Atlas 11
Human GBM tissue samples 11
Subtype assignment using NanoString nCounter Technology 11
Immunohistochemistry (IHC) 12
Image acquisition and quantification 12
Microglia/TAM shape analysis 14
Subtype prediction model 14
Statistics 15

Results **16**

Analysis of TCGA gene expression and survival data 16
Immune cell infiltration in human GBM and control samples 19
Tumor-associated macrophages and T cells in GBM subtypes 20
GBM subtype prediction model based on immune cell infiltration 25
TAM plasticity in the peri-tumor area of GBM 27

Discussion **29**

Bibliography **33**

Statutory Declaration **40**

Declaration of contribution to the top-journal publication **41**

Extract from the Journal Summary List **42**

Copy of the publication **50**

Curriculum Vitae Ioannis Kaffes **61**

List of Publications **63**

Acknowledgments **64**

List of Abbreviations

BMDM	Bone marrow-derived macrophage
CI	Confidence Interval
CL	Classical
CSF-1	Colony stimulating factor 1
EGFR	Epidermal Growth Factor Receptor
FFPE	Formalin-fixed, paraffin-embedded
FOXP3	Forkhead box P3
GBM	Glioblastoma
GBW	Gehan-Breslow-Wilcoxon test
G-CIMP	Glioma-CpG Island Methylator Phenotype
IBA1	Ionized calcium binding adapter molecule 1
IDH1	Isocitrate dehydrogenase 1
IHC	Immunohistochemistry
MC	Log-rank (Mantel-Cox) test
MCP	Monocyte chemoattractant protein
MES	Mesenchymal
NF1	Neurofibromin 1
NFκB	Nuclear factor kappa B
NL	Neural
PDGFB	Platelet-derived growth factor subunit B
PDGFRA	Platelet-derived growth factor receptor alpha
PN	Proneural
TAM	Tumor-associated macrophage
TCGA	The Cancer Genome Atlas
TNF	Tumor necrosis factor
T_{reg}	Regulatory T cell

Abstract

Background

Glioblastoma (GBM) is the most common and aggressive malignant primary brain tumor in adults. In order to improve our understanding of its complex pathophysiology and facilitate the advancement of personalized treatment options, recent research efforts have been undertaken to identify clinically relevant subgroups. As a result, three molecular subtypes have been consistently proposed: Proneural, Mesenchymal, and Classical GBM. Concurrently, constituents of the tumor microenvironment and their tumor-promoting properties have received growing attention. Special emphasis has been placed on tumor-associated macrophages (TAMs), a mixed cell population of activated brain-resident microglia and infiltrating monocyte-derived macrophages, as well as on different T cell populations. The aim of this study was to investigate how the cellular immune profile differs among the GBM subtypes.

Methods

Gene expression data obtained from The Cancer Genome Atlas (TCGA) were utilized to analyze subtype-specific differences in the immune profiles as well as the effects of marker levels on patient survival. Subsequently, human formalin-fixed, paraffin-embedded tumor samples were molecularly characterized using NanoString nCounter Technology and assigned to the three GBM subtypes. Automated immunohistochemical staining was performed for IBA1, a specific marker of TAMs, as well as CD3, CD8 and FOXP3, which represent different T cell-populations. Image analysis was then carried out to quantify immune cell infiltration. Furthermore, the marker combination was employed to develop a statistical model to predict the GBM subtype of a tumor based on its immune profile.

Results

TCGA and immunohistochemical analyses demonstrated stark differences in the composition of the immune cell compartment among the GBM subtypes. Mesenchymal GBM was characterized by significantly higher levels of TAMs as well as cytotoxic, helper and regulatory T cells. Moreover, a positive correlation between TAM and T cell infiltration was observed. Survival analysis based on TCGA data revealed a converse effect of *AIF1*, a gene encoding the TAM-marker IBA1, in Proneural and Mesenchymal GBM: in the former, high expression was associated with a worse prognosis, while

conferring a survival benefit in the latter. The subtype prediction-model was able to identify Mesenchymal tumors with a high sensitivity.

Conclusion

In order to improve patient outcomes, therapies that take into account tumor diversity are required. In this study, we demonstrated that GBMs are characterized not only by differences in their molecular profile, but also by a considerable heterogeneity of their immune microenvironment. This will hopefully contribute to the development of more effective immunotherapeutic approaches. Further research is required to illuminate the subtype-specific functional role that immune cells play in GBM pathogenesis.

Einleitung

Das Glioblastom ist der häufigste und aggressivste maligne hirneigene Tumor. Um das Verständnis der Pathophysiologie der Erkrankung zu verbessern sowie die Entwicklung personalisierter Therapiestrategien voranzutreiben, hat sich die Forschung intensiv um die Identifizierung klinisch relevanter Subgruppen bemüht. Eine der häufigsten Klassifizierungen basiert auf unterschiedlichen Genexpressionsprofilen und unterteilt Glioblastome in die Subtypen Proneural, Mesenchymal und Klassisch. Auch die zellulären Bestandteile des Tumormikromilieus und ihr Einfluss auf das Tumorwachstum sind zunehmend in den Fokus der wissenschaftlichen Arbeit gerückt. Insbesondere Tumor-assoziierte Makrophagen (TAM), eine gemischte Zellpopulation, welche sich aus aktivierten Mikroglia und eingewanderten Monozyten zusammensetzt, sowie T-Zellen spielen dabei eine übergeordnete Rolle. Das Ziel dieser Studie war es, die Immunzellinfiltration in den jeweiligen Subtypen des Glioblastoms zu charakterisieren.

Methodik

Genexpressionsdaten des The Cancer Genome Atlas (TCGA) wurden hinsichtlich der unterschiedlichen Immunprofile der Subtypen sowie ihrer Auswirkungen auf das Patientenüberleben analysiert. Zudem wurden Formalin-fixierte, Paraffin-eingebettete Gewebeproben mittels NanoString nCounter Technologie auf molekularer Ebene charakterisiert und den jeweiligen Subgruppen zugeordnet. Daraufhin wurde eine automatisierte immunhistochemische Färbung mit Antikörpern gegen IBA1, einem spezifischen Marker Tumor-assoziierter Makrophagen, sowie gegen die T-Zellproteine CD3, CD8 und FOXP3 durchgeführt. Die Quantifizierung der Immunzellinfiltration erfolgte mithilfe einer standardisierten Bildanalyse. Anhand der genannten Marker-Kombination wurde zudem ein mathematisches Modell entwickelt, mit welchem der Subtyp eines Glioblastoms vorhergesagt werde sollte.

Ergebnisse

Die Analysen sowohl auf Ebene der Genexpression als auch der Immunhistochemie offenbarten große Unterschiede in der Zusammensetzung der Immunzellen im Mikromilieu der Glioblastom-Subtypen. Mesenchymale Tumoren zeichneten sich durch eine signifikant erhöhte Infiltration von TAM sowie zytotoxischer, Helfer- und regulatorischer T-Zellen aus. Zudem wurde eine positive Korrelation zwischen TAM und

den jeweiligen T-Zellpopulationen festgestellt. In der Überlebenszeitanalyse, basierend auf Daten des TCGA, zeichnete sich ein gegenteiliger Effekt hoher *AIF1*-Werte, eines Gens, welches für IBA1 kodiert, in Proneuralen und Mesenchymalen Tumoren ab: in Ersteren waren hohe Expressionsniveaus mit einer schlechteren Prognose vergesellschaftet, während sie bei Letzteren mit einem Überlebensvorteil einhergingen. Das statistische Prädiktionsmodell konnte Mesenchymale Glioblastome mit einer hohen Wahrscheinlichkeit identifizieren.

Schlussfolgerungen

Um die Prognose von Glioblastom-Patienten zu verbessern sind gezielte Therapiestrategien notwendig, welche die Heterogenität der Entität berücksichtigen. Die Ergebnisse dieser Studie untermauern die Hypothese, dass es unterschiedliche Subtypen des Glioblastoms gibt, und dass diese sich nicht nur hinsichtlich ihres molekularen Profils, sondern auch in der Zusammensetzung ihres zellulären Immun-Mikromilieus unterscheiden. Diese Ergebnisse werden hoffentlich zur Entwicklung effektiverer Immuntherapien beitragen. Zukünftige Studien sind erforderlich, um die Subtyp-spezifischen Funktionen der Immunzellen in der Pathogenese des Glioblastoms zu beleuchten.

Synopsis

Introduction

Glioblastoma (GBM) is the most common and aggressive malignant primary brain tumor in the adult population (1). Despite an aggressive standard treatment protocol consisting of surgical resection followed by concomitant radiochemotherapy and adjuvant chemotherapy with the alkylating agent temozolomide, prognosis remains dismal, with a median survival rate of less than two years (2, 3). GBM used to be conceived of as a uniform entity with pseudopalisading necrosis, microvascular proliferation, high mitotic activity, and diffuse infiltration of the brain parenchyma constituting the main histological hallmarks (4). However, with the advent of high-throughput molecular sequencing, it has become increasingly evident that these tumors are defined by high levels of genetic and epigenetic heterogeneity. Thus, efforts have focused on identifying clinically relevant subgroups. The most widely recognized classification has been put forward by The Cancer Genome Atlas (TCGA) Research Network, which initially proposed four molecular subtypes, Proneural (PN), Mesenchymal (MES), Classical (CL), and Neural (NL) GBM, with the latter now being regarded as an artifact of healthy tissue sampling (5-7). The three remaining subtypes differ significantly with respect to their molecular profiles: While MES tumors harbor deletions of the region encoding the tumor suppressor *neurofibromin 1 (NF1)* and show an upregulation of genes related to the *TNF* and *NFκB* pathways, the CL subtype is characterized by a marked amplification of the *epidermal growth factor receptor (EGFR)* and significantly fewer mutations in the *TP53* gene. PN GBM is defined by an amplified *platelet-derived growth factor receptor alpha (PDGFRA).* A subset of PN tumors displays a glioma-CpG Island Methylator Phenotype (G-CIMP), which frequently harbors mutations in *isocitrate dehydrogenase 1 (IDH1*) and may indicate GBMs that arise from lower grade II or III gliomas and are associated with younger age as well as improved survival rates compared to primary GBMs (7, 8). Interestingly, single-cell analyses have revealed that multiple subtypes can co-exist within the same tumor (9). Nonetheless, the identified profiles represent the dominant subgroups at a given point in time.

Like other human cancers, GBMs consist not only of neoplastic tumor cells, but rather of complex cellular networks that also include, among others, stromal cell constituents such as endothelial cells, pericytes, fibroblasts, astrocytes, and immune cells. Collectively, these cells and their products are commonly referred to as the tumor

microenvironment (10). Neoplastic and non-neoplastic cells together form anatomically and functionally distinct niches, which drive tumor invasiveness and treatment resistance (11). Especially the role of immune cells in GBM has recently been the subject of growing research interest. One group of immune cells in particular, tumor-associated macrophages (TAMs), has generated excitement as a possible target for novel therapies. This mixed population of brain-resident yolk-sac derived activated microglia and infiltrating bone marrow-derived monocytes (BMDMs) has been shown to constitute up to 45% of cells in GBM (12, 13). They are recruited to gliomas through factors such as CSF-1 or members of the monocyte chemoattractant protein (MCP) family, which are secreted by neoplastic tumor cells (14, 15). In turn, these immune cells have been shown to switch to an immunosuppressive phenotype and are co-opted to promote GBM growth and invasion though reciprocal interactions with tumor cells (13, 16, 17).

The role of different T cell subpopulations in GBM, especially $CD4^+$ T helper, $CD8^+$ cytotoxic, and $FOXP3^+$ regulatory T cells, has also attracted significant attention, especially given the success of immunotherapeutic approaches in other entities such as malignant melanoma (18-21).

Given the relevance of the immune microenvironment in GBM pathogenesis, the question arises to what extent the GBM subtypes differ with respect to their immune cell composition. Previous gene expression studies have demonstrated an increased enrichment of immune response-related genes in human MES tumors compared to the other GBM subtypes (6, 7, 22, 23). Leveraging the RCAS/tv-a somatic gene transfer system, our group has been able to model the three GBM profiles by focusing on the main genetic driver mutations PDGFB-overexpression, NF1-silencing, and EGFRvIII-expression. With the help of these immunocompetent *mouse* models, which accurately recapitulate the transcription patterns associated with human PN, MES, and CL GBM respectively, we have demonstrated increased levels of TAMs in the MES subtype (24, 25).

The aim of this study was to investigate whether immune cell infiltration also differs among the distinct GBM subtypes in *human* GBM (26). Based on gene expression and immunohistochemical data, we identified significantly higher levels of TAMs and T cells in human MES GBM. Furthermore, we revealed that high levels of *AIF1*, a gene encoding the TAM-marker IBA1, have a positive effect on the survival of patients with MES tumors, but confer a survival disadvantage in PN GBM. Finally, we were able to

create a predictive model that accurately identified MES GBMs based on their immune cell profile.

Methods

The Cancer Genome Atlas

TCGA has compiled publicly available molecular information pertaining to a variety of cancer types, including GBM. Gene expression levels related to the cells of interest (*AIF1, CD8B, CD4, CD3G, FOXP3*) as well as survival data generated by TCGA were obtained in August 2016 using the following pathway from the tool "cBioPortal for Cancer Genomics": Cancer Study: Glioblastoma Multiforme (TCGA, Provisional), Genomic Profiles: mRNA Expression z-Scores (microarray) (27, 28). The analysis was limited to the 357 primary GBM samples with complete gene expression and subtype information as described by Verhaak et al (7). Of these, 69 belonged to the PN, 106 to the MES, and 101 to the CL subtype. 55 specimen that showed a NL signature and 26 that were G-CIMP positive were not included in the subtype-specific analysis. In order to determine the effect of high and low expression levels of the genes of interest on patient survival, these levels were defined as the average of all samples in a given subtype plus/minus 0.5 standard deviation.

Human GBM tissue samples

Formalin-fixed, paraffin-embedded (FFPE) human glioblastoma as well as post-mortem naïve brain samples along with anonymized clinical information were supplied for this study by Emory University, Memorial Sloan Kettering Cancer Center, Uppsala University, and the University of Washington Medical Center. The GBM specimen were graded by board-certified pathologists based on the 2007 World Health Organization Classification of Tumors of the Central Nervous System (4). Primary and recurrent tumor samples were included in the study. Ethical approval by institutional review boards was obtained prior to the commencement of the present study.

Subtype assignment using NanoString nCounter Technology

mRNA was extracted from the human GBM samples and gene expression levels were analyzed by NanoString nCounter Technology (NanoString Technologies, Seattle, U.S.A.) using custom-made probes for 152 genes designed by Cameron Brennan and Jason T. Huse (29). Subsequently, subtypes were assigned based on differential expression patterns.

Immunohistochemistry (IHC)

The FFPE GBM and control samples were sectioned at 5 micrometers. Automatic immunohistochemical staining was performed using the DISCOVERY XT platform (Ventana Medical Systems, Inc., Tucson, U.S.A) to ensure consistency. TAM and microglia were stained with antibodies that bind to ionized calcium binding adapter molecule 1 (IBA1), a protein involved in membrane ruffling and phagocytosis. Antibodies targeting CD3 and CD8, both of which function as co-receptors for the T cell receptor, stained the entire T cell population and cytotoxic T cells, respectively. Regulatory T (T_{reg}) cells were stained with the help of antibodies directed at forkhead box P3 (FOXP3), a key transcription factor for the development and function of these cells. Due to the absence of a validated and consistent antibody targeting CD4, the number of T helper cells was estimated to be the difference between $CD3^+$ and $CD8^+$ cells, as has been described previously (30). Since $CD8^+$ and $CD4^+$ cells are subsets of the $CD3^+$ T cell population, the former should individually or collectively not exceed the number of the latter. However, in six cases, the number of $CD8^+$ T cells was higher or the same as the $CD3^+$ T cell number. As a consequence, the $CD4^+$ T cell population was assumed to be equal to the $FOXP3^+$ T cell number, which constitutes a part of the $CD4^+$ population. The following primary antibodies were used: Anti-IBA1 (1:500, rabbit polyclonal, #019–19741, Wako Pure Chemical Ind., Ltd., Osaka, Japan); anti-human FOXP3, clone 259D (1:100, mouse monoclonal, #320202, BioLegend, San Diego, U.S.A); anti-human CD8, clone C8/144B (1:100, mousemonoclonal, code M7103, Dako, Glostrup, Denmark); antihuman CD3 (1:100, rabbit polyclonal, code A0452, Dako, Glostrup, Denmark).

Image acquisition and quantification

The stained tissue sections were converted into digital files with the help of the Nanozoomer 2.0HT (Hamamatsu Photonic K.K., Hamamatsu, Japan). In order to ensure consistency and reproducibility during cell quantification, a standardized process was performed on all tissue samples (Figure 1). First, based on the overall area of the sample, the total number of representative images to be obtained was calculated, with a minimum of five images per tumor. Second, given the high degree of intratumoral heterogeneity, each tissue sample was subdivided into regions of relatively homogeneous staining. These regions were then attributed a specific percentage of the total number of images as a function of their relative size. The image software Fiji was

employed for cell quantification (31). Given the abundance of TAMs in some GBM samples, it was not feasible to identify and quantify them individually. As a result, for this cell type the percentage of stained area per field was analyzed. $CD3^+$, $CD8^+$, and $FOXP3^+$ T cells on the other hand were quantified as the total number per field. A magnification of 20x was used to capture the selected images. Since two different screens were used for quantification, this equaled an area of 0.3828 mm^2 and 0.4263 mm^2. Pixel width of the images was 454 nanometers and final values were standardized to an area of one mm^2. Necrotic tumor areas as well as peritumor regions were excluded from the analysis. In order to avoid confounding effects, the investigators were blinded to the tissue subtype during the quantification process.

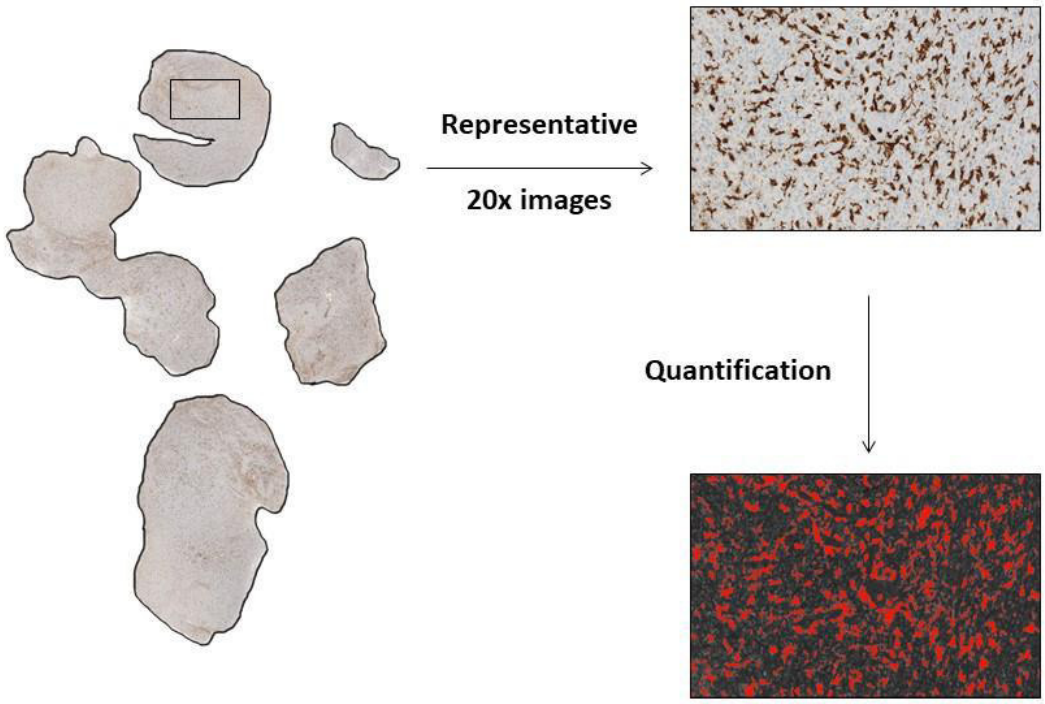

Figure 1. Schematic depicting the quantification process for $IBA1^+$ TAM. The tumor sections were subdivided into regions of homogeneous staining intensity (left), which were subsequently allocated a percentage of the overall number of images based on their relative size. Representative images were obtained and the percentage of IBA1-positive area (seen here as a red coloration) was quantified using the software Fiji.

Microglia/TAM shape analysis

Four GBM tissue samples stained for IBA1 with clearly demarcated adjacent non-tumor brain tissue were selected to further investigate changes in microglia/macrophage morphology. In every sample, three representative images of each of the three regions of interest were obtained: the tumor, non-tumor, and peri-tumor area. The latter was defined as a 20x field in which one half resembled tumor and the other non-tumor regions based on cellular density and macrophage morphology. Since the number of primary processes per $IBA1^+$ cell constitutes a surrogate parameter for TAM activation (low number of processes indicates a higher level of activation), they were counted and averaged in each field (32). It should be noted that the numbers of processes calculated in this study only represent relative values in a two-dimensional space. In order to further illustrate the changes in TAM density at the tumor edges, we created plot profiles measuring IBA1 staining intensity in four neighboring fields (non-tumor – peri-tumor – tumor – tumor) in each of the four GBM samples and plotted the mean and standard deviation with MatLab software (The MathWorks, Inc., Natick, U.S.A). Finally, IBA1 intensity was compared between the five control brain samples and the non-tumor tissue adjacent to eleven GBM samples to investigate differences in microglia density.

Subtype prediction model

On the basis of the markers used in this study, namely IBA1, CD3, CD8, and FOXP3, a threshold-based multinomial subtype prediction model with the three possible outcomes PN, MES, and CL was generated. Since the CD4 numbers were a function of CD3 and CD8, they were not included. Two independent binary regressions were fit for a training set of 29 samples, with the subtype PN as the reference. The two binary regression equations and the equation $P(CL) + P(MES) + P(PN) = 1$, with P indicating the probability for each subtype, were used to identify the parameter estimates.

Binary regression equations estimated from the multinomial model:

$$\log\left(\frac{\text{P(CL)}}{\text{P(PN)}}\right) = -0.7722 + 0.0350 * \text{IBA1} - 0.0067 * \text{FOXP3} + 0.0161 * \text{CD3} - 0.0040 * \text{CD8}$$

$$\log\left(\frac{\text{P(MES)}}{\text{P(PN)}}\right) = -8.8873 + 0.5496 * \text{IBA1} + 0.2417 * \text{FOXP3} + 0.0311 * \text{CD3} - 0.0594 * \text{CD8}$$

The parameters from the model were then applied to a test set of 21 samples to generate the predicted probabilities for each subtype. The subtype with the highest predicted probability was considered the predicted subtype in a given sample.

Statistics

All statistical analyses were performed and graphs created using GraphPad Prism 6.0b and 7.04 (GraphPad Software Inc., La Jolla, U.S.A). A one-way analysis of variance (ANOVA) as well as Tukey's multiple comparisons test were used when more than two groups were compared. The non-parametric Dunn's multiple comparisons test and two-tailed Mann-Whitney U test were applied for analyses with small samples sizes. Correlation analysis was performed with the Pearson correlation coefficient (r). The Logrank (Mantel-Cox) test and Gehan-Breslow-Wilcoxon test were used for survival analyses. Significance levels were indicated as follows: ns (not significant); * ($P < .05$); ** ($P < .01$); *** ($P < .001$); **** ($P < .0001$). Further information is included in the figure legends.

Results

Analysis of TCGA gene expression and survival data

As a first step in the analysis of differences in immune cell infiltration in the distinct GBM subtypes, we retrieved gene expression data from The Cancer Genome Atlas as described above and selected genes that encode the specific cell markers that were employed for the subsequent immunohistochemical analyses. The following genes were chosen: *AIF1*, which encodes the TAM-marker IBA1, *FOXP3* as a protein predominantly expressed by T_{regs}, the beta-chain of the cytotoxic T cell receptor CD8 (*CD8B*), *CD4* as a marker for T helper cells, and the gamma chain of CD3 (*CD3G*), a surface receptor expressed by all T cells. As was anticipated based on previously published data (22), *AIF1*, *CD3G,* and *CD4* were significantly upregulated in the MES tumors of our TCGA sample (Figure 2). We did not, however, see any difference with respect to the expression levels of *CD8B* or *FOXP3*.

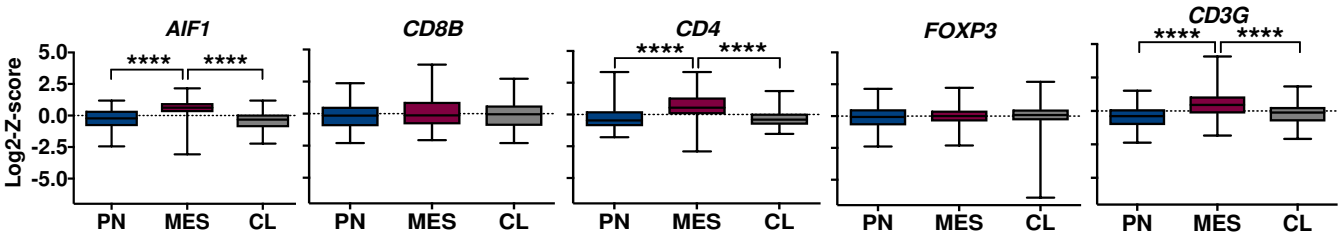

Figure 2. Box plots representing mRNA expression levels of immune-related genes in different GBM subtypes obtained from TCGA. The genes encode the following proteins: IBA1 (*AIF1*), beta-chain of CD8 (*CD8B*), CD4 (*CD4*), FOXP3 (*FOXP3*), as well as gamma-chain of CD3 (*CD3G*). MES GBM shows a significant upregulation of TAM, $CD3^+$ and $CD4^+$ T cell markers. Expression levels are depicted as Log2-Z-scores, with Z-scores describing the number of standard deviations that a value differs from the mean of a given population. Sixty-nine PN, 106 MES, and 101 CL samples were included (26).

In order to determine the impact of differences in expression levels and, by extension, cell infiltration, in general as well as within each subtype on overall survival, we divided the marker levels into groups of high and low expression. The combination of all TCGA GBM samples, including NL and G-CIMP-positive tumors, yielded a survival benefit for those patients with high expression levels of *CD3G* and *FOXP3* (Figure 3).

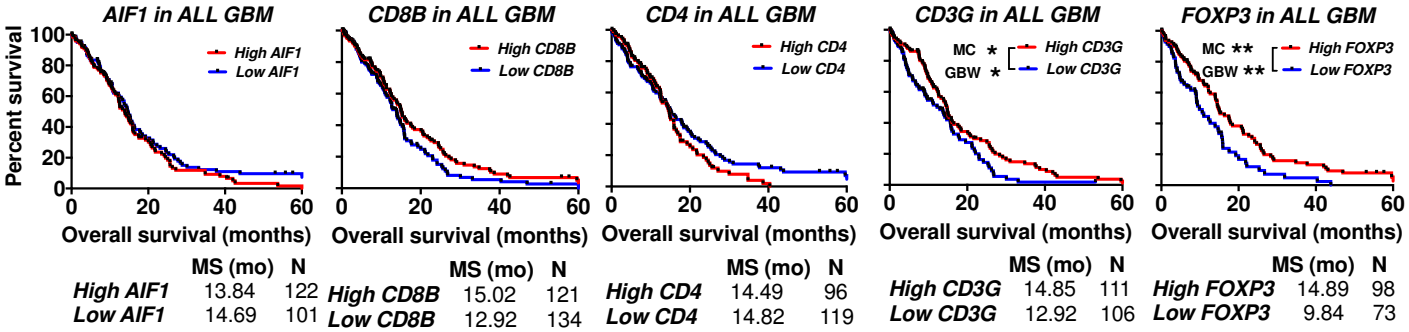

Figure 3. Kaplan-Meier curves displaying differences in overall survival of GBM patients independently of subtype, relative to high and low gene expression levels of immune-related markers. High expression of *FOXP3* and *CD3G* is associated with a significantly improved survival in GBM patients. Data obtained from TCGA. The average of all samples ± 0.5 standard deviations defined high and low expression levels. For practical purposes, the x-axis ends at 60 months**.** MS (mo) = Mean survival in months, MC = Log-rank (Mantel-Cox) test, GBW = Gehan-Breslow-Wilcoxon test (26).

In the PN subset, the only gene with prognostic value was *AIF1*, high levels of which were associated with a worse outcome (median survival high *AIF1*: 7.80 months, low *AIF1*: 10.56 months) (Figure 4).

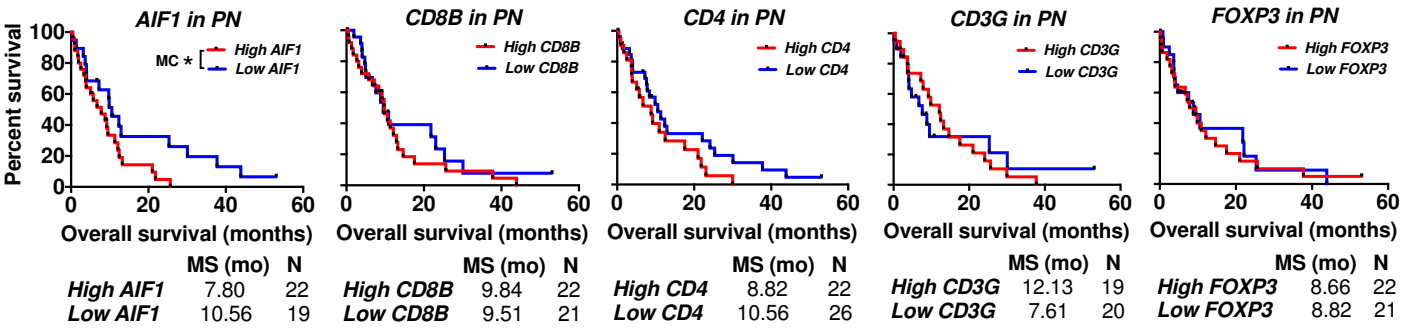

Figure 4. Kaplan-Meier curves comparing the overall survival of patients with PN GBM based on their expression levels of immune-related genes. Patients with low *AIF1* expression levels show a significantly longer overall survival compared to those with high *AIF1* levels (26).

Interestingly, high *AIF1* levels conferred a significant survival benefit in the MES cohort (high *AIF1*: 14.36 months, low *AIF1*: 7.31 months). The pan-T cell marker *CD3G* also proved beneficial in this subtype (median survival high *CD3G*: 14.36 months, low *CD3G*: 10.43 months) (Figure 5).

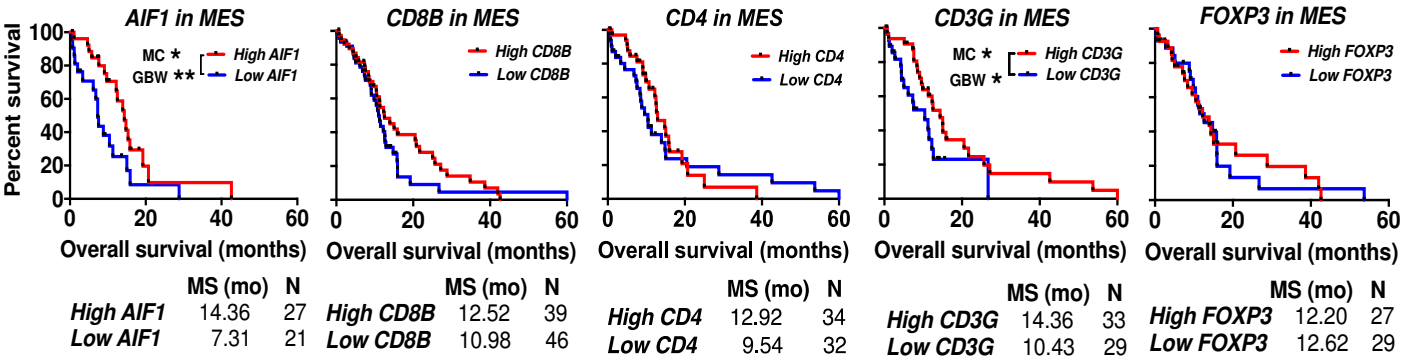

Figure 5. Kaplan-Meier curves comparing the overall survival of patients with MES GBM based on their expression levels of immune-related genes. High expression levels of *AIF1* and *CD3G* confer an improved survival in patients with MES GBM (26).

In CL samples, no survival differences were observed (Figure 6).

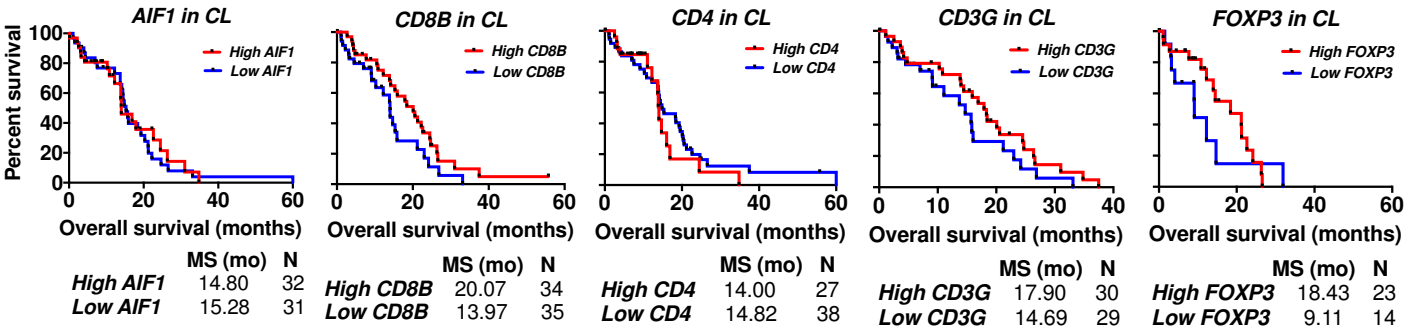

Figure 6. Kaplan-Meier curves showing no difference in overall survival of patients with CL GBM based on their expression levels of immune-related genes (26).

In conclusion, in our TCGA analysis we observed an increased expression of markers of TAM and certain T cell populations in MES GBM as well as distinct effects of expression levels related to immune cell constituents on patient survival.

Immune cell infiltration in human GBM and control samples

In spite of the unequivocal value of high-throughput sequencing endeavors, gene expression studies are associated with certain disadvantages such as the inability to characterize the cellular origin of expression patterns or to distinguish between an increasing number of cells and an upregulation of genes on a stable cell population. Hence, in a second step we pursued an immunohistochemical approach to further investigate immune cell infiltration in GBM and its subtypes.

Fifty-six GBM and five control brain samples were stained for IBA1, CD8, FOXP3, and CD3. Initially, all tumors were collectively compared against the controls (Figure 7). In GBM samples, IBA-positivity was significantly increased (mean area of all GBM samples: 13.9%, Controls: 3.9%) as were the numbers of $CD8^+$ (GBM: 20.3 cells/mm^2, controls: 2.2 cells/mm^2), $FOXP3^+$ (GBM: 3.1 cells/mm^2, controls: 0.25 cells/mm^2), and $CD3^+$ T cells (GBM: 44.6 cells/mm^2, controls: 1.3 cells/mm^2). The slightly lower number of $CD3^+$ T cells in the naïve brains compared to the $CD8^+$ T cell infiltration can be attributed to the very low levels of T cell infiltrates in healthy brains, likely beneath the level of accurate quantification using our method. We thus confirmed that our GBM samples were characterized by substantially higher levels of TAM and T cells. At the same time, we observed significant variability among the GBM samples. Consequently, we interrogated subtype-specific differences in immune cell infiltration.

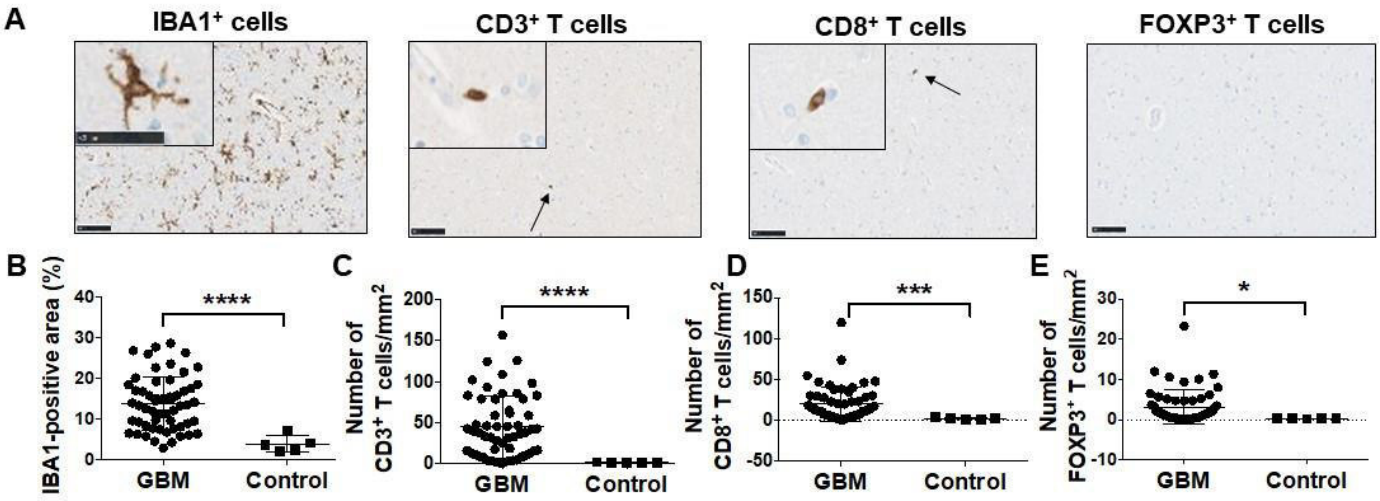

Figure 7. GBM shows increased infiltration of immune cells compared to naïve brain samples. (A) Representative images depicting different immune cell populations in naïve brains. (B – E) Dot plots demonstrating significantly higher infiltration of IBA1$^+$ microglia/TAM, CD3$^+$ T cells, CD8$^+$ cytotoxic, and FOXP3$^+$ regulatory T cells in GBM samples than in naïve control brains. Each dot represents an individual sample. Scale bars indicate lengths of 100 micrometers and 50 micrometers (inserted images) (26).

Tumor-associated macrophages and T cells in GBM subtypes

The subtype of the 56 GBM samples was determined using NanoString nCounter Technology as was described above. Thirteen tumors were found to be PN, 18 were characterized as MES, and 19 as CL. Six samples displayed a glioma-CpG Island Methylator Phenotype and were excluded from this analysis. In order to investigate TAM-infiltration in the three GBM subtypes, IBA1-positivity per mm^2 was analyzed as a surrogate parameter using Fiji. Quantification revealed significant differences, with an average of 19.2% IBA1-positive area in MES GBM compared to 9% in PN and 12% in CL tumors (Figure 8).

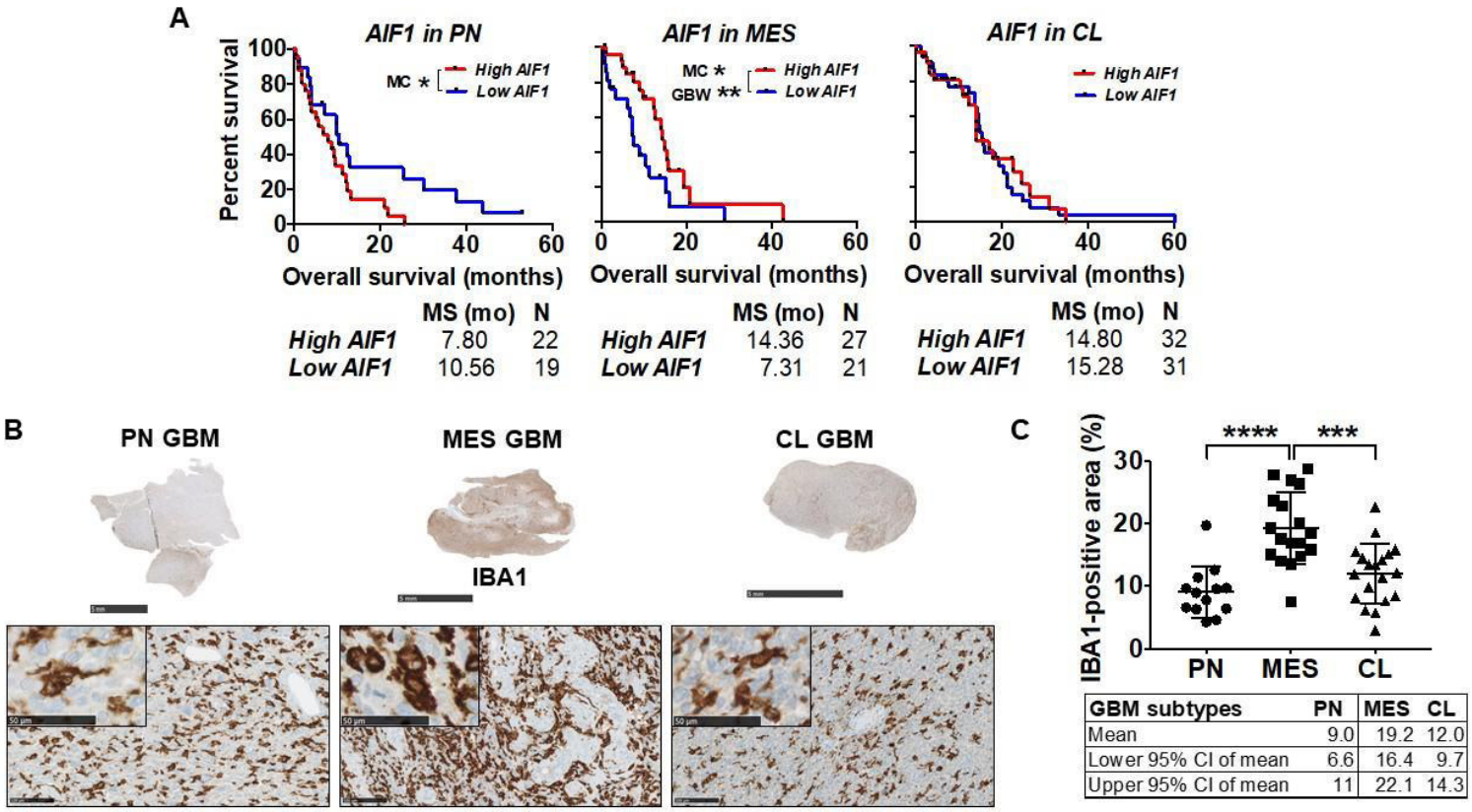

Figure 8. MES GBM is characterized by an increased presence of TAM compared to the PN and CL subtypes. (A) Kaplan-Meier curves created using data provided by TCGA comparing the effects of different expression levels of AIF1 on overall survival in GBM subtypes. High AIF1 expression levels confer a worse prognosis in the PN subtype, but bestow a survival benefit in MES tumors. No effect is seen in patients with CL GBM. High and low expression levels were defined as the average of all samples in each subtype ± 0.5 standard deviations. MC = Log-rank (Mantel-Cox) test, GBW = Gehan-Breslow Wilcoxon test. (B) Tumor sections (scale bars represent 5 mm) and representative images of GBM samples demonstrating differential immunohistochemical IBA1 staining among distinct GBM subtypes. IBA1 labels TAM in dark brown and nuclei are counterstained in blue using hematoxylin. Scale bar lengths correspond to 100 micrometers and 50 micrometers (inserted images). (C) Quantification of the percentage of IBA1-positive area in the different GBM subtypes. Each data point represents the average of one tumor. PN = Proneural, MES = Mesenchymal, CL = Classical (26).

Owing to their lower overall infiltration levels and clearer demarcation, T cells were quantified as absolute numbers per mm^2. Since CD3 labels all T cell populations, $CD3^+$ cells unsurprisingly were found at the highest rate of all T cells in each subtype. Their levels were significantly elevated in MES tumors (76.1 cells/mm^2) in comparison to PN and CL GBM (PN: 20.2 cells/mm^2, CL: 39 cells/mm^2). When specific T cell subpopulations were investigated, a similar pattern emerged. $CD4^+$ T cells, which constituted the most frequent subset, showed a markedly increased presence in the MES subtype (PN: 11.3, MES: 43.2, CL: 21.5 cells/mm^2), as did $CD8^+$ cells (PN: 9.4, MES: 32.9, CL: 18.6 cells/mm^2). It is worth noting, though, that the difference in $CD8^+$ numbers between MES and CL tumors was not significant ($p = 0.08$). The smallest subpopulation of T cells were $FOXP3^+$ T_{regs}, with MES GBM again demonstrating significantly higher levels (PN: 0.7, MES: 6.3, CL: 2.2 cells/mm^2) (Figure 9).

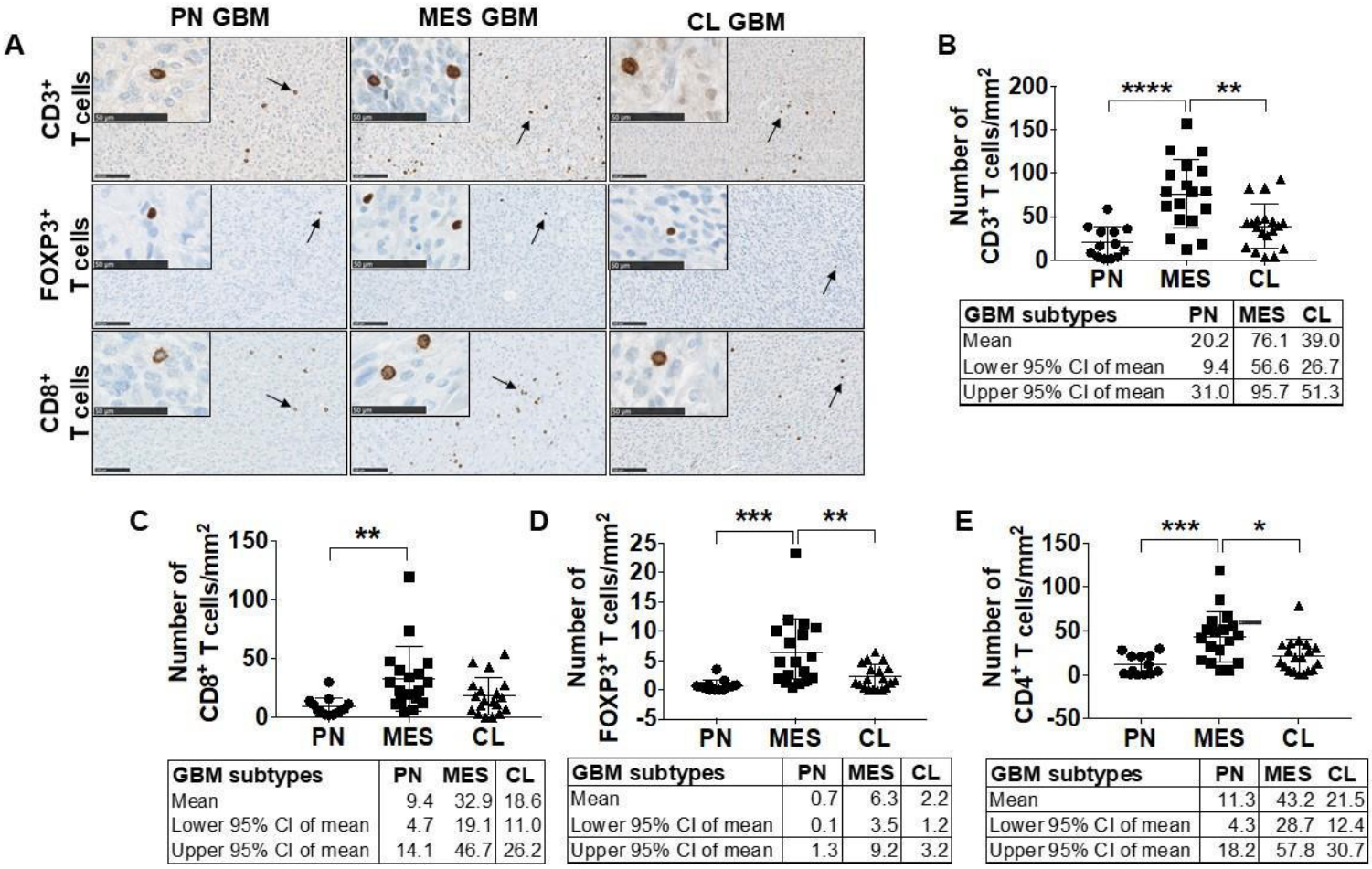

GBM subtypes	PN	MES	CL
Mean	20.2	76.1	39.0
Lower 95% CI of mean	9.4	56.6	26.7
Upper 95% CI of mean	31.0	95.7	51.3

GBM subtypes	PN	MES	CL
Mean	9.4	32.9	18.6
Lower 95% CI of mean	4.7	19.1	11.0
Upper 95% CI of mean	14.1	46.7	26.2

GBM subtypes	PN	MES	CL
Mean	0.7	6.3	2.2
Lower 95% CI of mean	0.1	3.5	1.2
Upper 95% CI of mean	1.3	9.2	3.2

GBM subtypes	PN	MES	CL
Mean	11.3	43.2	21.5
Lower 95% CI of mean	4.3	28.7	12.4
Upper 95% CI of mean	18.2	57.8	30.7

Figure 9. T cells preferentially infiltrate MES GBM. (A) Representative images depicting infiltrated CD3$^+$, FOXP3$^+$ and CD8$^+$ T cells (arrows) in different GBM subtypes. Scale bars indicate a length of 100 micrometers and 50 micrometers (inserted images). (B) Quantification of the number of CD3$^+$ cells reveals a higher density in MES GBM, with CD3 staining all T cells. (C) Infiltration of CD8$^+$ T cells differs significantly between the PN and MES subtypes. CD8$^+$ T cell numbers were also higher in MES than CL tumors, but not significantly ($p = .08$). (D, E) Dot plots demonstrating FOXP3$^+$ and CD4$^+$ T cells appear in significantly higher numbers in MES GBM. PN and CL GBM show similar levels of infiltration. The average of each tumor is represented by one data point (26).

Taken together, these findings provide evidence for a markedly increased infiltration of TAMs and T cells in the MES profile of GBM. This is further underscored by our data showing a significant positive correlation between IBA1$^+$ TAMs and all T cell populations, raising important questions regarding mechanism of infiltration and the interaction of these cell types (Figure 10).

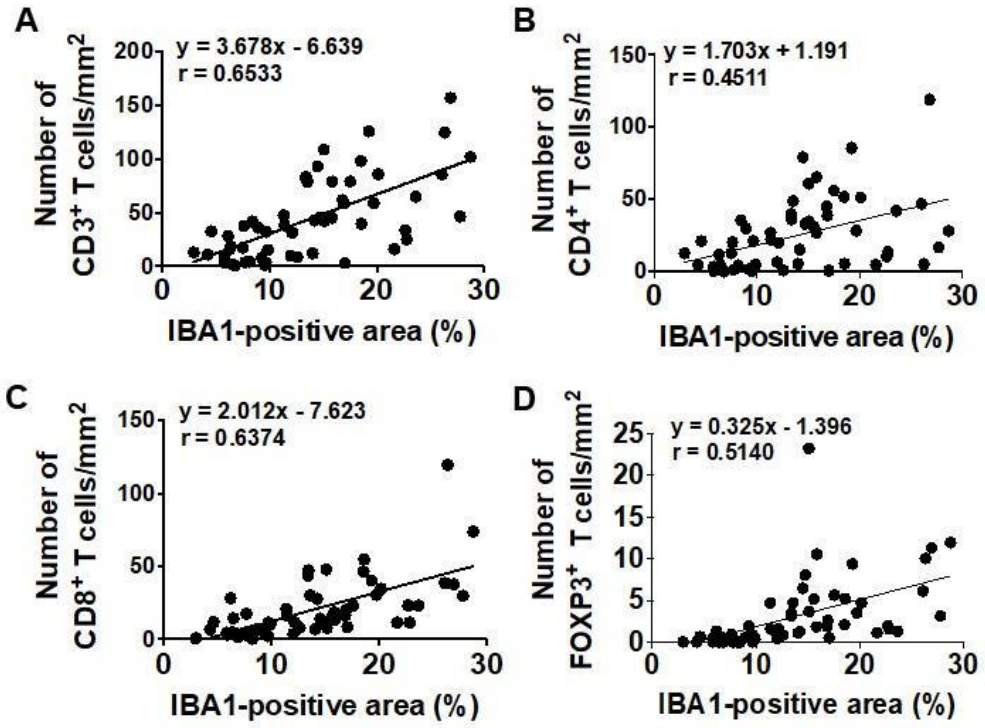

Figure 10. TAMs positively correlate with different T cell populations in GBM. (A) Pearson correlation demonstrating a positive association between the infiltration of TAM, represented by the percentage of IBA1-positive area, and the number of $CD3^+$ T cells. The same relationship can be observed with distinct subpopulations of T cells, including $CD4^+$ (B), $CD8^+$ (C) and $FOXP3^+$ T cells (D). r = Pearson r (26).

Lastly, we also compared the immune cell profile of the six G-CIMP-positive tumors in our set to all non-GCIMP tumors and were able to demonstrate significantly higher levels of $CD3^+$ T cells (G-CIMP: 20.2, non-G-CIMP: 47.5 cells/mm^2) and $CD4^+$ T cells (G-CIMP: 9.5, non-G-CIMP: 26.7 cells/mm^2) in the latter (Figure 11). However, caution should be exercised when interpreting these findings given the unequal group sizes.

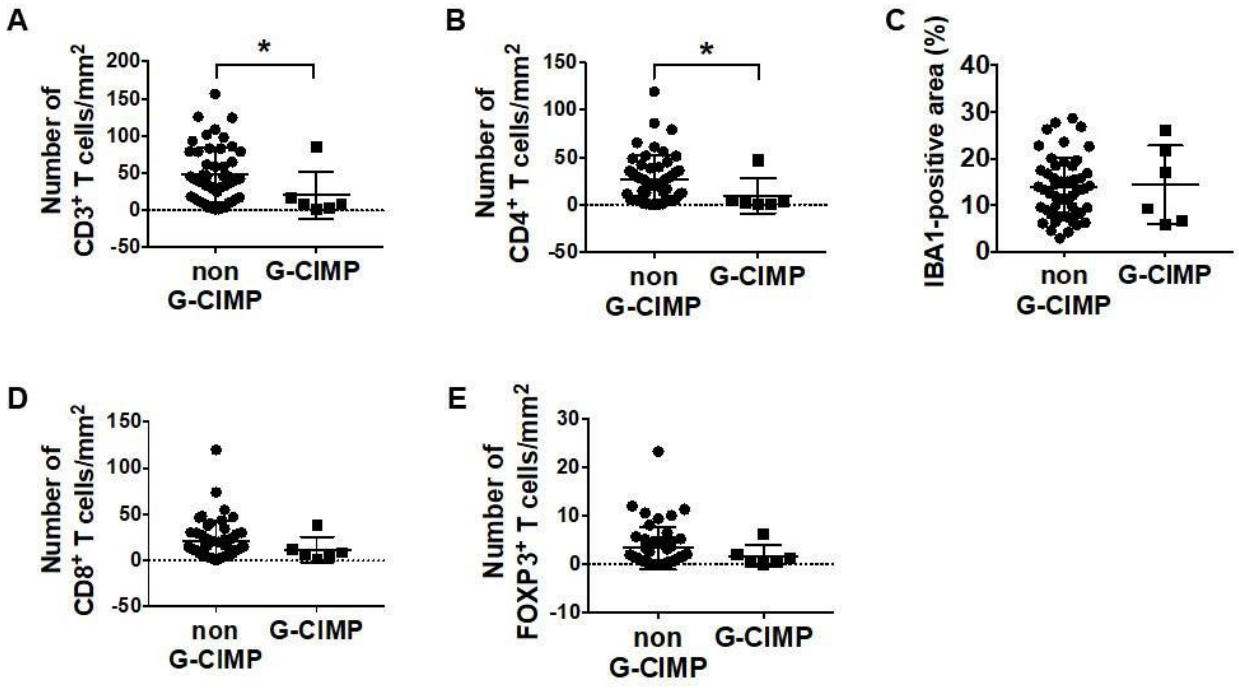

Figure 11. Infiltration of T cells is significantly decreased in GBM that display a glioma-CpG Island Methylator Phenotype (G-CIMP). (A, B) Quantification of the number of $CD3^+$ and $CD4^+$ T cells reveals a significantly lower density in G-CIMP GBM compared to non-G-CIMP tumors. (C, D, E) No significant differences can be seen in the infiltration of $IBA1^+$ TAM, $CD8^+$ and $FOXP3^+$ T cells. Each dot represents the average of one GBM sample. Mann-Whitney U test was performed due to the low sample number of G-CIMP tumors (26).

GBM subtype prediction model based on immune cell infiltration

Given the increased infiltration of distinct immune cell populations in the MES subtype, we investigated the possibility of using the markers IBA1, CD3, CD8, and FOXP3 to create the aforementioned multinomial model to predict the subgroup of our GBM samples. In the training set, which consisted of 9 PN, 11 MES, and 9 CL GBM samples, the subtype of 18 out of the 29 tumors (62.1%) was accurately identified. MES GBM were predicted correctly with a sensitivity of 90.9%, but PN and CL tumors only with a sensitivity of 55.5% and 33.3%. When applied to a test set consisting of 4 PN, 10 CL, and 7 MES tumors, 13 samples were correctly classified (61.9%). The model successfully predicted PN and MES samples with a sensitivity of 100% and 71.4%, respectively. It had less success with the CL subtype (sensitivity of 40%). Wald-type tests showed that no marker alone was significantly associated with any particular

subtype. While these results indicated the potential of the model to predict MES GBM using IHC, further validation is required with larger sample sizes and independent investigators (Tables 1-3).

Table 1. Sensitivity and specificity for each subtype within the multinomial model (Training set) (26).

Subtype	Sensitivity (95% CI)	Specificity (95% CI)
PN	55.5% (22.7%-84.7%)	75.0% (50.6%-90.4%)
CL	33.3% (9.0%-69.1%)	85.0% (61.1%-96.0%)
MES	90.9% (57.1%-99.5%)	83.3% (57.7%-95.6%)

CI: Confidence Interval, PN: Proneural, CL: Classical, MES: Mesenchymal

Table 2. Sensitivity and specificity for each subtype within the multinomial model (Test set) (26).

Subtype	Sensitivity (95% CI)	Specificity (95% CI)
PN	100.0% (39.6%,100.0%)	82.4% (55.8%, 95.3%)
CL	40.0% (13.7%, 72.6%)	90.9% (57.1%, 99.5%)
MES	71.4% (30.3%, 94.9%)	71.4% (42.0%, 90.4%)

CI: Confidence Interval, PN: Proneural, CL: Classical, MES: Mesenchymal

Table 3. Wald-type tests for each biomarker within the multinomial model (26).

Biomarker	p-value
IBA1	0.156
FOXP3	0.637
CD3	0.847
CD8	0.714

TAM plasticity in the peri-tumor area of GBM

GBMs are infiltrated by vast numbers of tumor-associated macrophages. Consequently, we decided to analyze the morphological changes that microglia/TAM undergo in the infiltrating zone in the manner described in the methods section. We observed a gradual decrease in the number of primary processes per cell as we moved from healthy brain into tumor tissue (non-tumor: 2.2, peri-tumor: 1.6, tumor: 1.1 primary processes/cell), indicating an increasing state of TAM/microglia activation. Furthermore, IBA1-positivity was analyzed in these fields and was shown to increase significantly in tumor direction (non-tumor: 5.9%, peri-tumor: 8.7%, tumor: 19.9%), which was also visualized by the plot profile in Figure 12. Taken together, these findings provide further evidence for the increased activation and infiltration of TAM in GBM compared to naïve brain tissue. In addition, IBA1-positivity was calculated in the adjacent brain tissue of eleven GBM samples and compared to the five control brain samples in order to investigate differences in microglia infiltration. However, no statistically significant variance was found (naïve control brains: 3.9%, non-tumor tissue of GBM samples: 4.5%).

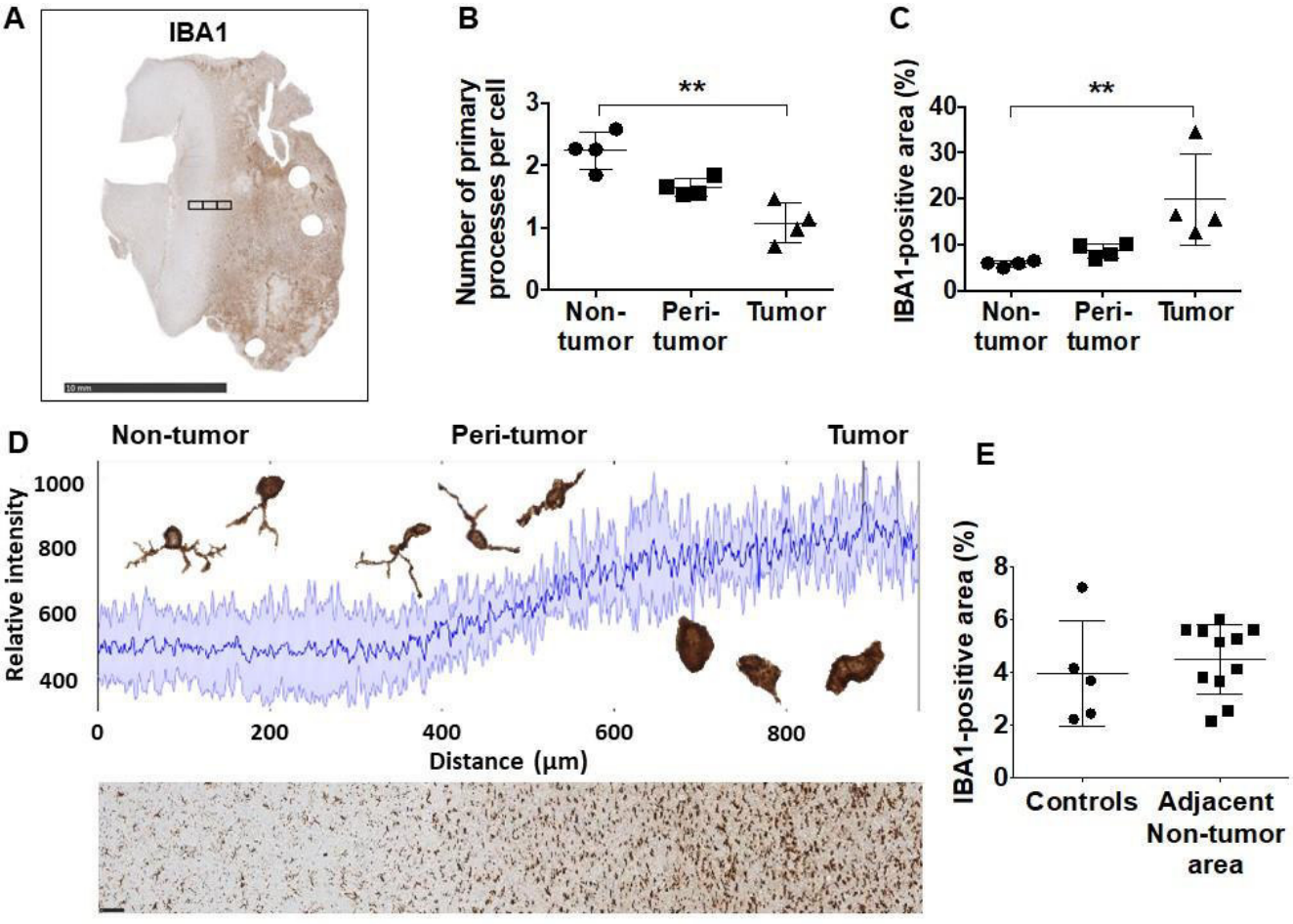

Figure 12. Tumor-associated macrophages (TAM) exhibit distinct morphologies in tumor and non-tumor regions. (A) Image of a GBM section with adjacent brain tissue stained with IBA1. The black rectangles represent images captured to quantify differences in the morphology of TAM in non-tumor (left), peri-tumor (mid), and tumor (right) areas, as well as changes in IBA1-positivity. Peri-tumor areas were defined as a field in which half of the area is non-tumor and the other half is tumor tissue based on macrophage morphology and cellular density. Scale bar corresponds to a length of 10 millimeters. (B) The number of primary processes per IBA1+ cell, a marker for macrophage shape and activation, changes incrementally from non-tumor to tumor areas. The data points represent average numbers of processes per cell in each area of different tumors. (C) Quantification shows the percentage area covered by IBA1+ TAM gradually increases from non-tumor to tumor areas, with each dot representing the average of one sample. Dunn´s multiple comparisons test was performed. (D) Plot profile demonstrating a gradual increase in relative IBA1 immunopositivity with increasing proximity to the tumor parenchyma. The solid dark blue line indicates mean intensity and the shades represent ± one standard deviation (n = 4 independent samples). Examples of TAM highlight their morphological plasticity. The section below the plot profile exemplifies the areas used for this analysis. Staining intensity increases from left (non-tumor) to right (tumor). The scale bar indicates a length of 100 micrometers. (E) Quantification of the percentage of the IBA1-positive area in control brains and non-tumor areas adjacent to GBM indicated no significant difference. Dots represent averages of each sample. Mann-Whitney U test was performed (26).

Discussion

Glioblastomas are almost uniformly fatal tumors and very little progress has been made in the last decades in improving median survival rates (2, 3), warranting advances on all clinical and scientific fronts. In this study, we provided evidence that GBMs are not only molecularly diverse, but also highly heterogeneous with respect to the composition of their cellular immune microenvironment (26). Leveraging TCGA data and immunohistochemical analyses, we were able to demonstrate significantly increased infiltration of tumor-associated macrophages as well as cytotoxic, helper, and regulatory T cells in the Mesenchymal GBM subtype.

In a study comparing MES with all non-MES tumors, Engler et al. also demonstrated increased TAM levels in the former, but unequal group sizes impeded a conclusive judgment (23). Beier et al. and Sorensen et al. likewise found higher TAM numbers in MES compared to PN tumors, but both had small sample sizes and determined the GBM subtype based solely on IHC markers (33, 34). Previous studies on T cell infiltration yielded less consistent results. While Prins et al. showed higher levels of $CD8^+$ and $CD3^+$ cells in MES vs. PN GBM, Han et al. did not find any subtype-specific differences in $CD4^+$ and $CD8^+$ T cell infiltration (19, 35). However, it is worth mentioning that both groups referred to different molecular classifications (7, 36). Our own study included adequate sample sizes and used validated NanoString nCounter Technology to identify the three recognized GBM subtypes (6). As a result, we were able to provide the first fairly comprehensive analysis of immune cell infiltration in human GBM based on immunohistochemistry rather than gene expression or flow cytometry data (6, 37). A recently published IHC study by Martinez-Lage et al. confirmed our findings of increased TAM and CD4+ T cell levels, but did not observe any differences in CD8+ T cell infiltration (38). Interestingly, we also did not detect a significant difference between the MES and CL subtype regarding the latter.

Furthermore, our analysis of TCGA revealed opposite survival effects of high AIF1-levels, which indicate increased TAM infiltration, in the MES and the PN subtypes. Patients with MES GBM and high expression survived significantly longer than those with low levels. In PN tumors this relationship was reversed. This interesting finding implies that TAM content is not in itself a predictor of survival. Rather, it raises questions regarding the specific composition of this diverse cell population and their functions in distinct GBM subtypes. Our RCAS/tv-a murine models have allowed our group to answer this question by using $Cx3cr1^{GFP/WT}$; $Ccr2^{RFP/WT}$ reporter mice (24, 39). Since

bone marrow-derived monocytes express both Cx3cr1 and Ccr2, but brain-resident microglia only the former, this approach allowed for the investigation of the specific composition of the TAM population in each subtype. The results showed that, while PN and CL GBM were mostly infiltrated by BMDMs, activated microglia constituted the main TAM population in MES tumors (24, 39). Whether or not this sufficiently explains the survival difference seen in this analysis is debatable. These findings do, however, highlight the need for further mechanistic studies investigating functional differences in these cell types. RNA analysis of genes differentially expressed by BMDMs and microglia in the PN GBM model demonstrated an increased enrichment of genes related to cell migration in the former, while microglia showed an upregulation of genes associated with metabolism and inflammation, underscoring their distinct functional contributions to gliomagenesis (39). The necessity for subtype-specific mechanistic analyses of TAMs in GBM is exemplified by a clinical trial using PLX3397, an inhibitor of the colony stimulating factor 1 receptor (CSF1R), a molecule involved in macrophage polarization, in non-stratified recurrent GBM patients, which did not demonstrate a significant improvement in progression-free survival, in spite of a striking therapeutic efficacy documented in mouse models of PN GBM (40, 41).

In addition, emphasis has to be put on understanding the mechanisms underlying differential immune cell infiltration and their interactions with each other as well as glioma cells. As an example, an experimental study demonstrated the ability of TAMs to attract $CCR4^+$ T_{reg} cells through the secretion of the chemokine CCL2, possibly explaining the significant correlation between the two seen in our cohort (42).

Our findings highlight the heterogeneity of GBMs and demonstrate the potential to stratify patients according to their specific tumor profile. We therefore created an affordable and easily applicable subtype prediction model. Even though an immediate adjustment of current therapeutic standards based on molecular profiles is not likely, studies such as a retrospective analysis of the AVAglio (Avastin in Glioblastoma) trial, which tested the addition of the VEGF inhibitor Bevacizumab in the first-line treatment of GBM and demonstrated a benefit in overall survival for patients with PN GBM as well as an improved progression-free survival for MES and PN GBM, highlight the fact that affordable and feasible patient stratification according to molecular subtypes is already relevant (43).

While the results of the present study paint a convincing picture of subtype-specific differences in GBM immune cell infiltration and are in line with other publications, it is associated with both technical and substantive limitations. The use of immunohistochemistry allows for the investigation of differences in immune profiles on the cellular level, a clear advantage to correlative gene expression studies. However, it also represents a rather subjective method, adding an element of uncertainty to the levels of cell infiltration described above. We addressed this challenge by creating a standardized pathway of image acquisition and by having a single investigator perform all of the image analyses, thus ensuring consistency. Furthermore, despite multiple attempts with various antibodies, we were not able to identify a reliable CD4 marker, leading us to estimate T helper cell levels by subtracting $CD8^+$ from $CD3^+$ T cell numbers. Even though this approach has been published before (30), it does constitute a relevant shortcoming. Our subtype-prediction model offers the intriguing possibility to identify MES tumors solely based on their immune cell content. Given the high costs and limited availability still associated with high-throughput molecular sequencing technologies, this approach might constitute a feasible alternative. Further studies involving larger sample sizes and multiple independent investigators are, however, required for validation. On a more substantive level, our study was not able to distinguish between the different TAM populations owing to a lack of validated markers in human samples. Moreover, the use of GBM subtype classifications has been criticized, especially since the recognition that multiple subtypes can co-exist within a single tumor (9). Nevertheless, this and other studies clearly demonstrate a biological correlate of these distinct gene expression patterns.

Future studies will have to further elucidate the reciprocal interactions of immune and neoplastic cells in the context of inter- and intratumoral molecular and cellular heterogeneity. Special emphasis ought to be placed on the mechanisms underlying the functions of the different TAM and T cell populations. Moreover, the role of the immune cell compartment in driving immune evasion and its subtype-specific therapeutic potential need to be investigated given the success immunotherapies have demonstrated in other entities. This is underscored by the disappointing results of immune checkpoint inhibitors in GBM, which have been partly attributed to the exhausted phenotype of intratumoral T cells and the immunosuppressive environment created by TAMs (44-47). Addressing these research questions will hopefully contribute to a better understanding of GBM pathogenesis and lead to the development of the next

generation of treatments that will give new hope to patients suffering from this dreadful disease.

Bibliography

1. Ostrom QT, Cioffi G, Gittleman H, Patil N, Waite K, Kruchko C, Barnholtz-Sloan JS. CBTRUS Statistical Report: Primary Brain and Other Central Nervous System Tumors Diagnosed in the United States in 2012-2016. Neuro-oncology. 2019;21(Suppl 5):v1-v100.

2. Stupp R, Taillibert S, Kanner A, Read W, Steinberg DM, Lhermitte B, Toms S, Idbaih A, Ahluwalia MS, Fink K, Di Meco F, Lieberman F, Zhu J-J, Stragliotto G, Tran DD, Brem S, Hottinger AF, Kirson ED, Lavy-Shahaf G, Weinberg U, Kim C-Y, Paek S-H, Nicholas G, Bruna J, Hirte H, Weller M, Palti Y, Hegi ME, Ram Z. Effect of Tumor-Treating Fields Plus Maintenance Temozolomide vs Maintenance Temozolomide Alone on Survival in Patients With Glioblastoma: A Randomized Clinical Trial. Jama. 2017;318(23):2306-16.

3. Stupp R, Mason WP, van den Bent MJ, Weller M, Fisher B, Taphoorn MJ, Belanger K, Brandes AA, Marosi C, Bogdahn U, Curschmann J, Janzer RC, Ludwin SK, Gorlia T, Allgeier A, Lacombe D, Cairncross JG, Eisenhauer E, Mirimanoff RO. Radiotherapy plus concomitant and adjuvant temozolomide for glioblastoma. The New England journal of medicine. 2005;352(10):987-96.

4. Louis DN, Ohgaki H, Wiestler OD, Cavenee WK, Burger PC, Jouvet A, Scheithauer BW, Kleihues P. The 2007 WHO classification of tumours of the central nervous system. Acta neuropathologica. 2007;114(2):97-109.

5. Gill BJ, Pisapia DJ, Malone HR, Goldstein H, Lei L, Sonabend A, Yun J, Samanamud J, Sims JS, Banu M, Dovas A, Teich AF, Sheth SA, McKhann GM, Sisti MB, Bruce JN, Sims PA, Canoll P. MRI-localized biopsies reveal subtype-specific differences in molecular and cellular composition at the margins of glioblastoma. Proceedings of the National Academy of Sciences of the United States of America. 2014;111(34):12550-5.

6. Wang Q, Hu X, Muller F, Kim H, Squatrito M, Millelsen T, Scarpace L, Barthel F, Lin Y-H, Satani N, Martinez-Ledesma E, Chang E, Olar A, Hu B, deCarvalho AC, Eskilsson E, Zheng S, Heimberger AB, Sulman EP, Nam D-H, Verhaak RGW. Tumor evolution of glioma intrinsic gene expression subtype associates with immunological changes in the microenvironment. bioRxiv. 2016.

7. Verhaak RG, Hoadley KA, Purdom E, Wang V, Qi Y, Wilkerson MD, Miller CR, Ding L, Golub T, Mesirov JP, Alexe G, Lawrence M, O'Kelly M, Tamayo P, Weir BA,

Gabriel S, Winckler W, Gupta S, Jakkula L, Feiler HS, Hodgson JG, James CD, Sarkaria JN, Brennan C, Kahn A, Spellman PT, Wilson RK, Speed TP, Gray JW, Meyerson M, Getz G, Perou CM, Hayes DN. Integrated genomic analysis identifies clinically relevant subtypes of glioblastoma characterized by abnormalities in PDGFRA, IDH1, EGFR, and NF1. Cancer cell. 2010;17(1):98-110.

8. Noushmehr H, Weisenberger DJ, Diefes K, Phillips HS, Pujara K, Berman BP, Pan F, Pelloski CE, Sulman EP, Bhat KP, Verhaak RG, Hoadley KA, Hayes DN, Perou CM, Schmidt HK, Ding L, Wilson RK, Van Den Berg D, Shen H, Bengtsson H, Neuvial P, Cope LM, Buckley J, Herman JG, Baylin SB, Laird PW, Aldape K. Identification of a CpG island methylator phenotype that defines a distinct subgroup of glioma. Cancer cell. 2010;17(5):510-22.

9. Patel AP, Tirosh I, Trombetta JJ, Shalek AK, Gillespie SM, Wakimoto H, Cahill DP, Nahed BV, Curry WT, Martuza RL, Louis DN, Rozenblatt-Rosen O, Suva ML, Regev A, Bernstein BE. Single-cell RNA-seq highlights intratumoral heterogeneity in primary glioblastoma. Science (New York, NY). 2014;344(6190):1396-401.

10. Charles NA, Holland EC, Gilbertson R, Glass R, Kettenmann H. The brain tumor microenvironment. Glia. 2012;60(3):502-14.

11. Hambardzumyan D, Bergers G. Glioblastoma: Defining Tumor Niches. Trends in cancer. 2015;1(4):252-65.

12. Morantz RA, Wood GW, Foster M, Clark M, Gollahon K. Macrophages in experimental and human brain tumors. Part 2: studies of the macrophage content of human brain tumors. Journal of neurosurgery. 1979;50(3):305-11.

13. Hambardzumyan D, Gutmann DH, Kettenmann H. The role of microglia and macrophages in glioma maintenance and progression. Nature neuroscience. 2016;19(1):20-7.

14. Coniglio SJ, Eugenin E, Dobrenis K, Stanley ER, West BL, Symons MH, Segall JE. Microglial stimulation of glioblastoma invasion involves epidermal growth factor receptor (EGFR) and colony stimulating factor 1 receptor (CSF-1R) signaling. Molecular medicine (Cambridge, Mass). 2012;18(1):519-27.

15. Okada M, Saio M, Kito Y, Ohe N, Yano H, Yoshimura S, Iwama T, Takami T. Tumor-associated macrophage/microglia infiltration in human gliomas is correlated with MCP-3, but not MCP-1. International journal of oncology. 2009;34(6):1621-7.

16. Markovic DS, Vinnakota K, Chirasani S, Synowitz M, Raguet H, Stock K, Sliwa M, Lehmann S, Kälin R, van Rooijen N, Holmbeck K, Heppner FL, Kiwit J, Matyash V,

Lehnardt S, Kaminska B, Glass R, Kettenmann H. Gliomas induce and exploit microglial MT1-MMP expression for tumor expansion. Proceedings of the National Academy of Sciences of the United States of America. 2009;106(30):12530-5.
17. Wu A, Wei J, Kong LY, Wang Y, Priebe W, Qiao W, Sawaya R, Heimberger AB. Glioma cancer stem cells induce immunosuppressive macrophages/microglia. Neuro-oncology. 2010;12(11):1113-25.
18. Hodi FS, O'Day SJ, McDermott DF, Weber RW, Sosman JA, Haanen JB, Gonzalez R, Robert C, Schadendorf D, Hassel JC, Akerley W, van den Eertwegh AJ, Lutzky J, Lorigan P, Vaubel JM, Linette GP, Hogg D, Ottensmeier CH, Lebbé C, Peschel C, Quirt I, Clark JI, Wolchok JD, Weber JS, Tian J, Yellin MJ, Nichol GM, Hoos A, Urba WJ. Improved survival with ipilimumab in patients with metastatic melanoma. The New England journal of medicine. 2010;363(8):711-23.
19. Prins RM, Soto H, Konkankit V, Odesa SK, Eskin A, Yong WH, Nelson SF, Liau LM. Gene expression profile correlates with T-cell infiltration and relative survival in glioblastoma patients vaccinated with dendritic cell immunotherapy. Clinical cancer research : an official journal of the American Association for Cancer Research. 2011;17(6):1603-15.
20. Rutledge WC, Kong J, Gao J, Gutman DA, Cooper LA, Appin C, Park Y, Scarpace L, Mikkelsen T, Cohen ML, Aldape KD, McLendon RE, Lehman NL, Miller CR, Schniederjan MJ, Brennan CW, Saltz JH, Moreno CS, Brat DJ. Tumor-infiltrating lymphocytes in glioblastoma are associated with specific genomic alterations and related to transcriptional class. Clinical cancer research : an official journal of the American Association for Cancer Research. 2013;19(18):4951-60.
21. Yang I, Tihan T, Han SJ, Wrensch MR, Wiencke J, Sughrue ME, Parsa AT. CD8+ T-cell infiltrate in newly diagnosed glioblastoma is associated with long-term survival. Journal of clinical neuroscience : official journal of the Neurosurgical Society of Australasia. 2010;17(11):1381-5.
22. Doucette T, Rao G, Rao A, Shen L, Aldape K, Wei J, Dziurzynski K, Gilbert M, Heimberger AB. Immune heterogeneity of glioblastoma subtypes: extrapolation from the cancer genome atlas. Cancer immunology research. 2013;1(2):112-22.
23. Engler JR, Robinson AE, Smirnov I, Hodgson JG, Berger MS, Gupta N, James CD, Molinaro A, Phillips JJ. Increased microglia/macrophage gene expression in a subset of adult and pediatric astrocytomas. PloS one. 2012;7(8):e43339.

24. Chen Z, Herting CJ, Ross JL, Gabanic B, Puigdelloses Vallcorba M, Szulzewsky F, Wojciechowicz ML, Cimino PJ, Ezhilarasan R, Sulman EP, Ying M, Ma'ayan A, Read RD, Hambardzumyan D. Genetic driver mutations introduced in identical cell-of-origin in murine glioblastoma reveal distinct immune landscapes but similar response to checkpoint blockade. Glia. 2020.
25. Herting CJ, Chen Z, Pitter KL, Szulzewsky F, Kaffes I, Kaluzova M, Park JC, Cimino PJ, Brennan C, Wang B, Hambardzumyan D. Genetic driver mutations define the expression signature and microenvironmental composition of high-grade gliomas. Glia. 2017;65(12):1914-26.
26. Kaffes I, Szulzewsky F, Chen Z, Herting CJ, Gabanic B, Velázquez Vega JE, Shelton J, Switchenko JM, Ross JL, McSwain LF, Huse JT, Westermark B, Nelander S, Forsberg-Nilsson K, Uhrbom L, Maturi NP, Cimino PJ, Holland EC, Kettenmann H, Brennan CW, Brat DJ, Hambardzumyan D. Human Mesenchymal glioblastomas are characterized by an increased immune cell presence compared to Proneural and Classical tumors. Oncoimmunology. 2019;8(11):e1655360.
27. Cerami E, Gao J, Dogrusoz U, Gross BE, Sumer SO, Aksoy BA, Jacobsen A, Byrne CJ, Heuer ML, Larsson E, Antipin Y, Reva B, Goldberg AP, Sander C, Schultz N. The cBio cancer genomics portal: an open platform for exploring multidimensional cancer genomics data. Cancer discovery. 2012;2(5):401-4.
28. Gao J, Aksoy BA, Dogrusoz U, Dresdner G, Gross B, Sumer SO, Sun Y, Jacobsen A, Sinha R, Larsson E, Cerami E, Sander C, Schultz N. Integrative analysis of complex cancer genomics and clinical profiles using the cBioPortal. Science signaling. 2013;6(269):pl1.
29. Kastenhuber ER, Huse JT, Berman SH, Pedraza A, Zhang J, Suehara Y, Viale A, Cavatore M, Heguy A, Szerlip N, Ladanyi M, Brennan CW. Quantitative assessment of intragenic receptor tyrosine kinase deletions in primary glioblastomas: their prevalence and molecular correlates. Acta neuropathologica. 2014;127(5):747-59.
30. Lohr J, Ratliff T, Huppertz A, Ge Y, Dictus C, Ahmadi R, Grau S, Hiraoka N, Eckstein V, Ecker RC, Korff T, von Deimling A, Unterberg A, Beckhove P, Herold-Mende C. Effector T-cell infiltration positively impacts survival of glioblastoma patients and is impaired by tumor-derived TGF-β. Clinical cancer research : an official journal of the American Association for Cancer Research. 2011;17(13):4296-308.
31. Schindelin J, Arganda-Carreras I, Frise E, Kaynig V, Longair M, Pietzsch T, Preibisch S, Rueden C, Saalfeld S, Schmid B, Tinevez JY, White DJ, Hartenstein V,

Eliceiri K, Tomancak P, Cardona A. Fiji: an open-source platform for biological-image analysis. Nature methods. 2012;9(7):676-82.
32. Kettenmann H, Hanisch UK, Noda M, Verkhratsky A. Physiology of microglia. Physiological reviews. 2011;91(2):461-553.
33. Beier CP, Kumar P, Meyer K, Leukel P, Bruttel V, Aschenbrenner I, Riemenschneider MJ, Fragoulis A, Rummele P, Lamszus K, Schulz JB, Weis J, Bogdahn U, Wischhusen J, Hau P, Spang R, Beier D. The cancer stem cell subtype determines immune infiltration of glioblastoma. Stem cells and development. 2012;21(15):2753-61.
34. Sorensen MD, Dahlrot RH, Boldt HB, Hansen S, Kristensen BW. Tumour-associated microglia/macrophages predict poor prognosis in high-grade gliomas and correlate with an aggressive tumour subtype. Neuropathology and applied neurobiology. 2018;44(2):185-206.
35. Han S, Zhang C, Li Q, Dong J, Liu Y, Huang Y, Jiang T, Wu A. Tumour-infiltrating CD4(+) and CD8(+) lymphocytes as predictors of clinical outcome in glioma. British journal of cancer. 2014;110(10):2560-8.
36. Phillips HS, Kharbanda S, Chen R, Forrest WF, Soriano RH, Wu TD, Misra A, Nigro JM, Colman H, Soroceanu L, Williams PM, Modrusan Z, Feuerstein BG, Aldape K. Molecular subclasses of high-grade glioma predict prognosis, delineate a pattern of disease progression, and resemble stages in neurogenesis. Cancer cell. 2006;9(3):157-73.
37. Gabrusiewicz K, Rodriguez B, Wei J, Hashimoto Y, Healy LM, Maiti SN, Thomas G, Zhou S, Wang Q, Elakkad A, Liebelt BD, Yaghi NK, Ezhilarasan R, Huang N, Weinberg JS, Prabhu SS, Rao G, Sawaya R, Langford LA, Bruner JM, Fuller GN, Bar-Or A, Li W, Colen RR, Curran MA, Bhat KP, Antel JP, Cooper LJ, Sulman EP, Heimberger AB. Glioblastoma-infiltrated innate immune cells resemble M0 macrophage phenotype. JCI insight. 2016;1(2).
38. Martinez-Lage M, Lynch TM, Bi Y, Cocito C, Way GP, Pal S, Haller J, Yan RE, Ziober A, Nguyen A, Kandpal M, O'Rourke DM, Greenfield JP, Greene CS, Davuluri RV, Dahmane N. Immune landscapes associated with different glioblastoma molecular subtypes. Acta neuropathologica communications. 2019;7(1):203.
39. Chen Z, Feng X, Herting CJ, Garcia VA, Nie K, Pong WW, Rasmussen R, Dwivedi B, Seby S, Wolf SA, Gutmann DH, Hambardzumyan D. Cellular and Molecular

Identity of Tumor-Associated Macrophages in Glioblastoma. Cancer research. 2017;77(9):2266-78.
40. Butowski N, Colman H, De Groot JF, Omuro AM, Nayak L, Wen PY, Cloughesy TF, Marimuthu A, Haidar S, Perry A, Huse J, Phillips J, West BL, Nolop KB, Hsu HH, Ligon KL, Molinaro AM, Prados M. Orally administered colony stimulating factor 1 receptor inhibitor PLX3397 in recurrent glioblastoma: an Ivy Foundation Early Phase Clinical Trials Consortium phase II study. Neuro-oncology. 2016;18(4):557-64.
41. Pyonteck SM, Akkari L, Schuhmacher AJ, Bowman RL, Sevenich L, Quail DF, Olson OC, Quick ML, Huse JT, Teijeiro V, Setty M, Leslie CS, Oei Y, Pedraza A, Zhang J, Brennan CW, Sutton JC, Holland EC, Daniel D, Joyce JA. CSF-1R inhibition alters macrophage polarization and blocks glioma progression. Nature medicine. 2013;19(10):1264-72.
42. Chang AL, Miska J, Wainwright DA, Dey M, Rivetta CV, Yu D, Kanojia D, Pituch KC, Qiao J, Pytel P, Han Y, Wu M, Zhang L, Horbinski CM, Ahmed AU, Lesniak MS. CCL2 Produced by the Glioma Microenvironment Is Essential for the Recruitment of Regulatory T Cells and Myeloid-Derived Suppressor Cells. Cancer research. 2016;76(19):5671-82.
43. Sandmann T, Bourgon R, Garcia J, Li C, Cloughesy T, Chinot OL, Wick W, Nishikawa R, Mason W, Henriksson R, Saran F, Lai A, Moore N, Kharbanda S, Peale F, Hegde P, Abrey LE, Phillips HS, Bais C. Patients With Proneural Glioblastoma May Derive Overall Survival Benefit From the Addition of Bevacizumab to First-Line Radiotherapy and Temozolomide: Retrospective Analysis of the AVAglio Trial. Journal of clinical oncology : official journal of the American Society of Clinical Oncology. 2015;33(25):2735-44.
44. Jackson CM, Choi J, Lim M. Mechanisms of immunotherapy resistance: lessons from glioblastoma. Nature Immunology. 2019;20(9):1100-9.
45. Reardon DA, Brandes AA, Omuro A, Mulholland P, Lim M, Wick A, Baehring J, Ahluwalia MS, Roth P, Bähr O, Phuphanich S, Sepulveda JM, De Souza P, Sahebjam S, Carleton M, Tatsuoka K, Taitt C, Zwirtes R, Sampson J, Weller M. Effect of Nivolumab vs Bevacizumab in Patients With Recurrent Glioblastoma: The CheckMate 143 Phase 3 Randomized Clinical Trial. JAMA Oncology. 2020;6(7):1003-10.
46. Wei J, Marisetty A, Schrand B, Gabrusiewicz K, Hashimoto Y, Ott M, Grami Z, Kong L-Y, Ling X, Caruso H, Zhou S, Wang YA, Fuller GN, Huse J, Gilboa E, Kang N, Huang X, Verhaak R, Li S, Heimberger AB. Osteopontin mediates glioblastoma-

associated macrophage infiltration and is a potential therapeutic target. The Journal of Clinical Investigation. 2019;129(1):137-49.
47. Wen PY, Weller M, Lee EQ, Alexander BM, Barnholtz-Sloan JS, Barthel FP, Batchelor TT, Bindra RS, Chang SM, Chiocca EA, Cloughesy TF, DeGroot JF, Galanis E, Gilbert MR, Hegi ME, Horbinski C, Huang RY, Lassman AB, Le Rhun E, Lim M, Mehta MP, Mellinghoff IK, Minniti G, Nathanson D, Platten M, Preusser M, Roth P, Sanson M, Schiff D, Short SC, Taphoorn MJB, Tonn J-C, Tsang J, Verhaak RGW, von Deimling A, Wick W, Zadeh G, Reardon DA, Aldape KD, van den Bent MJ. Glioblastoma in adults: a Society for Neuro-Oncology (SNO) and European Society of Neuro-Oncology (EANO) consensus review on current management and future directions. Neuro-oncology. 2020;22(8):1073-113.

Statutory Declaration

"I, Ioannis Kaffes, by personally signing this document in lieu of an oath, hereby affirm that I prepared the submitted dissertation on the topic "Subtype-specific differences in the cellular glioblastoma microenvironment", independently and without the support of third parties, and that I used no other sources and aids than those stated.
All parts which are based on the publications or presentations of other authors, either in letter or in spirit, are specified as such in accordance with the citing guidelines. The sections on methodology (in particular regarding practical work, laboratory regulations, statistical processing) and results (in particular regarding figures, charts and tables) are exclusively my responsibility.

Furthermore, I declare that I have correctly marked all of the data, the analyses, and the conclusions generated from data obtained in collaboration with other persons, and that I have correctly marked my own contribution and the contributions of other persons (cf. declaration of contribution). I have correctly marked all texts or parts of texts that were generated in collaboration with other persons.

My contributions to any publications to this dissertation correspond to those stated in the below joint declaration made together with the supervisor. All publications created within the scope of the dissertation comply with the guidelines of the ICMJE (International Committee of Medical Journal Editors; www.icmje.org) on authorship. In addition, I declare that I shall comply with the regulations of Charité – Universitätsmedizin Berlin on ensuring good scientific practice.

I declare that I have not yet submitted this dissertation in identical or similar form to another Faculty.

The significance of this statutory declaration and the consequences of a false statutory declaration under criminal law (Sections 156, 161 of the German Criminal Code) are known to me."

July 25, 2020
Date Signature

Declaration of contribution to the top-journal publication

Ioannis Kaffes contributed the following to the below listed publication:

Publication 1: Ioannis Kaffes, Frank Szulzewsky, Zhihong Chen, Cameron J. Herting, Ben Gabanic, José E. Velázquez Vega, Jennifer Shelton, Jeffrey M. Switchenko, James L. Ross, Leon F. McSwain, Jason T. Huse, Bengt Westermark, Sven Nelander, Karin Forsberg-Nilsson, Lene Uhrbom, Naga Prathyusha Maturi, Patrick J. Cimino, Eric C. Holland, Helmut Kettenmann, Cameron W. Brennan, Daniel J. Brat & Dolores Hambardzumyan, Human Mesenchymal glioblastomas are characterized by an increased immune cell presence compared to Proneural and Classical tumors, Oncoimmunology, 2019.

Contribution:

- Planning of the study (together with Dolores Hambardzumyan and Helmut Kettenmann)
- Development of the methodology
- Retrieval and analysis of data provided by The Cancer Genome Atlas
- Image analysis and quantification
- Statistical analysis (exception: the statistical prediction model was developed by Jeffrey M. Switchenko based on our data)
- Drafting and revision of the manuscript
- All tables and figures were based on data collected by and were created by Ioannis Kaffes, with the exception of Figure 4, which was created by Dave Schumick based on our data, and the plot profile in Figure 5, which was generated by Zhihong Chen

_____

Signature of doctoral candidate

Journal Data Filtered By: **Selected JCR Year: 2017** Selected Editions: SCIE,SSCI Selected Categories: **"ONCOLOGY"** Selected Category Scheme: WoS

Gesamtanzahl: 222 Journale

Rank	Full Journal Title	Total Cites	Journal Impact Factor	Eigenfactor Score
1	CA-A CANCER JOURNAL FOR CLINICIANS	28,839	244.585	0.066030
2	NATURE REVIEWS CANCER	50,407	42.784	0.079730
3	LANCET ONCOLOGY	44,961	36.418	0.136440
4	JOURNAL OF CLINICAL ONCOLOGY	156,474	26.303	0.285130
5	Nature Reviews Clinical Oncology	8,354	24.653	0.026110
6	Cancer Discovery	11,896	24.373	0.065350
7	CANCER CELL	35,217	22.844	0.096910
8	JAMA Oncology	5,707	20.871	0.027770
9	ANNALS OF ONCOLOGY	38,738	13.926	0.095780
10	JNCI-Journal of the National Cancer Institute	37,933	11.238	0.052550
11	Journal of Thoracic Oncology	15,010	10.336	0.033280
12	CLINICAL CANCER RESEARCH	81,859	10.199	0.132210
13	SEMINARS IN CANCER BIOLOGY	6,330	10.198	0.010740
14	LEUKEMIA	25,265	10.023	0.059580
15	NEURO-ONCOLOGY	10,930	9.384	0.030350
16	Cancer Immunology Research	4,361	9.188	0.021180
17	CANCER RESEARCH	139,291	9.130	0.130190
18	Journal for ImmunoTherapy of Cancer	1,675	8.374	0.007130
19	BIOCHIMICA ET BIOPHYSICA ACTA-REVIEWS ON CANCER	5,276	8.220	0.009300
20	Blood Cancer Journal	1,804	8.125	0.007660
21	CANCER TREATMENT REVIEWS	7,870	8.122	0.015820
22	Molecular Cancer	10,301	7.776	0.017280
23	INTERNATIONAL JOURNAL OF CANCER	51,800	7.360	0.071870
24	Journal of Hematology & Oncology	4,098	7.333	0.009750
25	EUROPEAN JOURNAL OF CANCER	29,883	7.191	0.050170
26	ONCOGENE	66,411	6.854	0.075960
27	CANCER	68,221	6.537	0.074740
28	CANCER LETTERS	29,311	6.491	0.042280
29	Journal of the National Comprehensive Cancer Network	5,143	6.471	0.017530
30	Advances in Cancer Research	2,343	6.422	0.003690
31	JOURNAL OF PATHOLOGY	16,156	6.253	0.024060

Rank	Full Journal Title	Total Cites	Journal Impact Factor	Eigenfactor Score
32	Therapeutic Advances in Medical Oncology	1,020	6.238	0.002650
33	JOURNAL OF EXPERIMENTAL & CLINICAL CANCER RESEARCH	5,661	6.217	0.008740
34	BREAST CANCER RESEARCH	11,022	6.142	0.020000
35	Pigment Cell & Melanoma Research	4,430	6.115	0.007840
36	Clinical Epigenetics	2,172	6.091	0.007720
37	CANCER AND METASTASIS REVIEWS	6,106	6.081	0.006870
38	BRITISH JOURNAL OF CANCER	46,723	5.922	0.065130
39	STEM CELLS	21,694	5.587	0.035680
40	INTERNATIONAL JOURNAL OF RADIATION ONCOLOGY BIOLOGY PHYSICS	46,595	5.554	0.055060
41	OncoImmunology	5,963	5.503	0.020500
42	MOLECULAR CANCER THERAPEUTICS	19,211	5.365	0.031690
43	ENDOCRINE-RELATED CANCER	7,114	5.331	0.012410
44	Cancers	3,897	5.326	0.008990
45	ONCOLOGIST	11,433	5.306	0.020480
46	Molecular Oncology	4,529	5.264	0.013160
47	CARCINOGENESIS	21,776	5.072	0.021960
48	Gastric Cancer	4,290	5.045	0.006460
49	NEOPLASIA	6,801	4.994	0.008860
50	SEMINARS IN ONCOLOGY	5,409	4.942	0.007270
52	CELLULAR ONCOLOGY	1,322	4.761	0.002020
53	Oncogenesis	1,348	4.722	0.004480
54	ORAL ONCOLOGY	8,949	4.636	0.013760
55	Cancer Biology & Medicine	816	4.607	0.002330
56	MOLECULAR CANCER RESEARCH	7,834	4.597	0.013490
57	JOURNAL OF ENVIRONMENTAL SCIENCE AND HEALTH PART C-ENVIRONMENTAL CARCINOGENESIS & ECOTOXICOLOGY REVIEWS	895	4.586	0.000810
58	CANCER EPIDEMIOLOGY BIOMARKERS & PREVENTION	19,976	4.554	0.029440
59	GYNECOLOGIC ONCOLOGY	23,652	4.540	0.034310
60	Journal of Oncology	1,573	4.528	0.002410
61	BONE MARROW TRANSPLANTATION	12,506	4.497	0.020810

Rank	Full Journal Title	Total Cites	Journal Impact Factor	Eigenfactor Score
62	CRITICAL REVIEWS IN ONCOLOGY HEMATOLOGY	6,956	4.495	0.012190
63	LUNG CANCER	11,340	4.486	0.019070
64	Frontiers in Oncology	6,599	4.416	0.024250
65	CANCER SCIENCE	11,994	4.372	0.016230
66	CANCER IMMUNOLOGY IMMUNOTHERAPY	7,509	4.225	0.012830
67	Clinical Lung Cancer	2,360	4.204	0.005450
68	PROSTATE CANCER AND PROSTATIC DISEASES	2,022	4.099	0.004890
69	CANCER GENE THERAPY	2,928	4.044	0.003610
70	SEMINARS IN RADIATION ONCOLOGY	2,480	4.027	0.003620
71	Cancer Prevention Research	5,348	4.021	0.011930
72	American Journal of Cancer Research	3,246	3.998	0.008250
73	Cancer Cell International	2,393	3.960	0.004960
74	Targeted Oncology	1,008	3.877	0.002560
75	CANCER CYTOPATHOLOGY	2,544	3.866	0.004380
76	Clinical Colorectal Cancer	1,264	3.861	0.002620
77	ANNALS OF SURGICAL ONCOLOGY	26,592	3.857	0.053440
78	MOLECULAR CARCINOGENESIS	5,244	3.851	0.007630
79	JOURNAL OF IMMUNOTHERAPY	3,093	3.826	0.004590
80	BIODRUGS	1,435	3.825	0.002460
81	Chinese Journal of Cancer	2,161	3.822	0.003960
82	Journal of Cancer Survivorship	2,225	3.713	0.007530
83	Cancer Management and Research	739	3.702	0.001970
84	Molecular Therapy-Oncolytics	254	3.690	0.000830
85	Chinese Journal of Cancer Research	1,128	3.689	0.002420
86	EJSO	7,996	3.688	0.014750
87	CURRENT OPINION IN ONCOLOGY	2,962	3.653	0.005630
88	BREAST CANCER RESEARCH AND TREATMENT	19,709	3.605	0.037840
89	CURRENT TREATMENT OPTIONS IN ONCOLOGY	1,242	3.562	0.002670
90	CANCER JOURNAL	2,899	3.519	0.005390
91	INVESTIGATIONAL NEW DRUGS	4,450	3.502	0.009350
92	Journal of Bone Oncology	280	3.500	0.000860

Rank	Full Journal Title	Total Cites	Journal Impact Factor	Eigenfactor Score
93	ACTA ONCOLOGICA	7,207	3.473	0.013060
94	CLINICAL & EXPERIMENTAL METASTASIS	3,506	3.455	0.004330
94	PSYCHO-ONCOLOGY	10,201	3.455	0.019830
96	INTERNATIONAL JOURNAL OF HYPERTHERMIA	3,350	3.440	0.004040
97	AMERICAN JOURNAL OF CLINICAL ONCOLOGY-CANCER CLINICAL TRIALS	4,247	3.424	0.005470
98	ONCOLOGY-NEW YORK	2,317	3.398	0.003800
99	UROLOGIC ONCOLOGY-SEMINARS AND ORIGINAL INVESTIGATIONS	4,787	3.397	0.013310
100	CANCER BIOLOGY & THERAPY	7,577	3.373	0.008280
101	GENES CHROMOSOMES & CANCER	5,116	3.362	0.006970
102	Journal of Geriatric Oncology	895	3.359	0.003320
103	Journal of Gynecologic Oncology	957	3.340	0.002260
104	INTERNATIONAL JOURNAL OF ONCOLOGY	15,493	3.333	0.022360
105	EXPERIMENTAL CELL RESEARCH	19,420	3.309	0.019610
106	BMC CANCER	24,272	3.288	0.053080
107	JOURNAL OF CANCER RESEARCH AND CLINICAL ONCOLOGY	7,401	3.282	0.010800
108	Journal of Cancer	2,710	3.249	0.006580
109	Cancer Research and Treatment	1,873	3.230	0.004340
110	Cancer Medicine	3,123	3.202	0.011220
111	HEMATOLOGICAL ONCOLOGY	1,007	3.193	0.002060
112	Surgical Oncology Clinics of North America	1,139	3.178	0.002150
113	ONCOLOGY RESEARCH	1,573	3.143	0.001570
114	World Journal of Gastrointestinal Oncology	1,069	3.140	0.002520
115	MELANOMA RESEARCH	2,356	3.135	0.004620
116	Current Oncology Reports	1,650	3.122	0.003720
117	HEMATOLOGY-ONCOLOGY CLINICS OF NORTH AMERICA	2,277	3.098	0.004500
118	Translational Oncology	1,791	3.071	0.004510
119	American Journal of Translational Research	3,677	3.061	0.008470
120	JOURNAL OF NEURO-ONCOLOGY	10,858	3.060	0.017330
121	CLINICAL ONCOLOGY	3,372	3.055	0.005910
122	CANCER IMAGING	1,150	3.016	0.002250

Rank	Full Journal Title	Total Cites	Journal Impact Factor	Eigenfactor Score
123	ONCOLOGY REPORTS	16,599	2.976	0.026240
124	JOURNAL OF MAMMARY GLAND BIOLOGY AND NEOPLASIA	2,148	2.963	0.001760
125	BREAST	4,249	2.951	0.009830
126	MEDICAL ONCOLOGY	6,893	2.920	0.014110
127	Photodiagnosis and Photodynamic Therapy	2,180	2.895	0.002610
128	Cancer Epidemiology	2,796	2.888	0.009460
129	EUROPEAN JOURNAL OF CANCER PREVENTION	2,615	2.886	0.004090
129	JOURNAL OF SURGICAL ONCOLOGY	9,904	2.886	0.015910
131	Radiation Oncology	5,157	2.862	0.013540
132	CANCER CHEMOTHERAPY AND PHARMACOLOGY	9,993	2.808	0.013730
133	CANCER CAUSES & CONTROL	7,748	2.728	0.013250
134	Clinical Breast Cancer	2,079	2.703	0.004190
135	SUPPORTIVE CARE IN CANCER	10,484	2.676	0.024580
136	INTEGRATIVE CANCER THERAPIES	1,368	2.657	0.002150
137	OncoTargets and Therapy	5,065	2.656	0.012570
138	PEDIATRIC BLOOD & CANCER	9,907	2.646	0.023240
139	LEUKEMIA & LYMPHOMA	8,243	2.644	0.016110
140	CURRENT CANCER DRUG TARGETS	2,900	2.626	0.003180
141	International Journal of Clinical Oncology	2,667	2.610	0.005740
142	Hormones & Cancer	600	2.581	0.001630
143	Thoracic Cancer	698	2.569	0.001850
144	SURGICAL ONCOLOGY-OXFORD	1,675	2.558	0.002780
145	Anti-Cancer Agents in Medicinal Chemistry	3,142	2.556	0.004730
146	Clinical Genitourinary Cancer	1,628	2.539	0.005000
147	Brain Tumor Pathology	639	2.535	0.001120
148	Journal of Oncology Practice	2,508	2.509	0.010490
148	Recent Patents on Anti-Cancer Drug Discovery	575	2.509	0.001020
150	STRAHLENTHERAPIE UND ONKOLOGIE	2,820	2.459	0.004600
151	Journal of Breast Cancer	853	2.456	0.002130
152	Cancer Genomics & Proteomics	869	2.432	0.001440
153	Breast Journal	2,522	2.424	0.003710
154	EUROPEAN JOURNAL OF CANCER CARE	2,576	2.409	0.004330

Rank	Full Journal Title	Total Cites	Journal Impact Factor	Eigenfactor Score
155	Cancer Biomarkers	1,354	2.392	0.002170
155	Clinical & Translational Oncology	2,326	2.392	0.004250
157	Current Hematologic Malignancy Reports	658	2.388	0.002310
158	JAPANESE JOURNAL OF CLINICAL ONCOLOGY	4,535	2.370	0.006790
159	Future Oncology	3,829	2.369	0.007750
160	Cancer Genetics	1,108	2.351	0.003490
161	Expert Review of Anticancer Therapy	2,720	2.347	0.004490
162	LEUKEMIA RESEARCH	6,335	2.319	0.009870
163	Clinical Lymphoma Myeloma & Leukemia	1,944	2.308	0.005070
164	NUTRITION AND CANCER-AN INTERNATIONAL JOURNAL	5,412	2.261	0.004970
165	Brachytherapy	1,991	2.227	0.004240
166	INTERNATIONAL JOURNAL OF GYNECOLOGICAL CANCER	6,915	2.192	0.010820
167	Journal of Adolescent and Young Adult Oncology	370	2.167	0.001020
168	Journal of Contemporary Brachytherapy	556	2.146	0.001210
169	Infectious Agents and Cancer	806	2.123	0.001930
170	CANCER INVESTIGATION	2,775	2.053	0.002530
171	Breast Care	708	2.028	0.001790
172	Frontiers of Medicine	764	2.027	0.002060
172	Hereditary Cancer in Clinical Practice	288	2.027	0.000660
174	Cancer Control	1,473	2.009	0.002510
175	CHEMOTHERAPY	1,485	2.000	0.001060
176	Current Oncology	1,975	1.967	0.005130
177	Familial Cancer	1,593	1.943	0.003840
178	PATHOLOGY & ONCOLOGY RESEARCH	2,068	1.935	0.003600
179	Molecular Medicine Reports	11,289	1.922	0.027690
180	JOURNAL OF ONCOLOGY PHARMACY PRACTICE	934	1.908	0.001990
181	ANTI-CANCER DRUGS	3,659	1.869	0.003860
182	ANTICANCER RESEARCH	19,602	1.865	0.022440
183	CANCER NURSING	2,927	1.844	0.004280
184	European Journal of Oncology Nursing	2,088	1.812	0.004630
185	World Journal of Surgical Oncology	4,007	1.792	0.009360
186	ONCOLOGY NURSING FORUM	3,329	1.785	0.004330
187	Breast Cancer	1,392	1.772	0.002310
188	Journal of BUON	1,412	1.766	0.002580

Rank	Full Journal Title	Total Cites	Journal Impact Factor	Eigenfactor Score
189	Radiology and Oncology	706	1.722	0.001390
190	NEOPLASMA	1,804	1.696	0.002430
191	CANCER BIOTHERAPY AND RADIOPHARMACEUTICALS	1,619	1.682	0.001850
192	Seminars in Oncology Nursing	771	1.667	0.001010
193	Oncology Letters	8,967	1.664	0.021820
194	TECHNOLOGY IN CANCER RESEARCH & TREATMENT	1,671	1.646	0.002360
195	CURRENT PROBLEMS IN CANCER	373	1.609	0.000630
196	Analytical Cellular Pathology	322	1.574	0.000460
197	JOURNAL OF CANCER EDUCATION	1,626	1.547	0.003840
198	Progress in Tumor Research	41	1.524	0.000180
199	Asia-Pacific Journal of Clinical Oncology	729	1.494	0.001970
199	Oncology Research and Treatment	467	1.494	0.001340
201	UHOD-Uluslararasi Hematoloji-Onkoloji Dergisi	276	1.492	0.000570
202	JOURNAL OF CHEMOTHERAPY	1,326	1.490	0.001770
203	INTERNATIONAL JOURNAL OF BIOLOGICAL MARKERS	810	1.449	0.000900
204	Journal of Gastric Cancer	532	1.400	0.001180
205	International Journal of Clinical and Experimental Pathology	9,246	1.396	0.022890
206	TUMORI JOURNAL	2,115	1.304	0.002450
207	Journal of Pediatric Oncology Nursing	892	1.294	0.001000
208	BIRTH DEFECTS RESEARCH PART B-DEVELOPMENTAL AND REPRODUCTIVE TOXICOLOGY	847	1.244	0.000720
209	Translational Cancer Research	618	1.200	0.002200
210	PEDIATRIC HEMATOLOGY AND ONCOLOGY	1,168	1.154	0.001720
211	Cancer Radiotherapie	812	1.128	0.001010
212	JOURNAL OF PEDIATRIC HEMATOLOGY ONCOLOGY	3,585	1.060	0.004890
213	FOLIA BIOLOGICA	538	1.044	0.000610
214	Medical Dosimetry	725	0.886	0.001100
215	Clinical Journal of Oncology Nursing	1,389	0.881	0.002030
216	Journal of Cancer Research and Therapeutics	1,825	0.842	0.003520
217	BULLETIN DU CANCER	1,016	0.840	0.000850

Rank	Full Journal Title	Total Cites	Journal Impact Factor	Eigenfactor Score
218	INDIAN JOURNAL OF CANCER	1,082	0.658	0.001640
219	EUROPEAN JOURNAL OF GYNAECOLOGICAL ONCOLOGY	1,361	0.617	0.001410
220	Onkologe	148	0.193	0.000130
221	Psycho-Oncologie	33	0.085	0.000030
222	Oncologie	61	0.035	0.000080

Ioannis Kaffes, Frank Szulzewsky, Zhihong Chen, Cameron J. Herting, Ben Gabanic, José E. Velázquez Vega, Jennifer Shelton, Jeffrey M. Switchenko, James L. Ross, Leon F. McSwain, Jason T. Huse, Bengt Westermark, Sven Nelander, Karin Forsberg-Nilsson, Lene Uhrbom, Naga Prathyusha Maturi, Patrick. J. Cimino, Eric C. Holland, Helmut Kettenmann, Cameron W. Brennan, Daniel J. Brat & Dolores Hambardzumyan (2019). Human Mesenchymal glioblastomas are characterized by an increased immune cell presence compared to Proneural and Classical tumors, OncoImmunology, 8:11, https://doi.org/10.1080/2162402X.2019.1655360.

Ioannis Kaffes, Frank Szulzewsky, Zhihong Chen, Cameron J. Herting, Ben Gabanic, José E. Velázquez Vega, Jennifer Shelton, Jeffrey M. Switchenko, James L. Ross, Leon F. McSwain, Jason T. Huse, Bengt Westermark, Sven Nelander, Karin Forsberg-Nilsson, Lene Uhrbom, Naga Prathyusha Maturi, Patrick. J. Cimino, Eric C. Holland, Helmut Kettenmann, Cameron W. Brennan, Daniel J. Brat & Dolores Hambardzumyan (2019). Human Mesenchymal glioblastomas are characterized by an increased immune cell presence compared to Proneural and Classical tumors, OncoImmunology, 8:11, https://doi.org/10.1080/2162402X.2019.1655360.

Ioannis Kaffes, Frank Szulzewsky, Zhihong Chen, Cameron J. Herting, Ben Gabanic, José E. Velázquez Vega, Jennifer Shelton, Jeffrey M. Switchenko, James L. Ross, Leon F. McSwain, Jason T. Huse, Bengt Westermark, Sven Nelander, Karin Forsberg-Nilsson, Lene Uhrbom, Naga Prathyusha Maturi, Patrick. J. Cimino, Eric C. Holland, Helmut Kettenmann, Cameron W. Brennan, Daniel J. Brat & Dolores Hambardzumyan (2019). Human Mesenchymal glioblastomas are characterized by an increased immune cell presence compared to Proneural and Classical tumors, OncoImmunology, 8:11, https://doi.org/10.1080/2162402X.2019.1655360.

Ioannis Kaffes, Frank Szulzewsky, Zhihong Chen, Cameron J. Herting, Ben Gabanic, José E. Velázquez Vega, Jennifer Shelton, Jeffrey M. Switchenko, James L. Ross, Leon F. McSwain, Jason T. Huse, Bengt Westermark, Sven Nelander, Karin Forsberg-Nilsson, Lene Uhrbom, Naga Prathyusha Maturi, Patrick. J. Cimino, Eric C. Holland, Helmut Kettenmann, Cameron W. Brennan, Daniel J. Brat & Dolores Hambardzumyan (2019). Human Mesenchymal glioblastomas are characterized by an increased immune cell presence compared to Proneural and Classical tumors, OncoImmunology, 8:11, https://doi.org/10.1080/2162402X.2019.1655360.

Ioannis Kaffes, Frank Szulzewsky, Zhihong Chen, Cameron J. Herting, Ben Gabanic, José E. Velázquez Vega, Jennifer Shelton, Jeffrey M. Switchenko, James L. Ross, Leon F. McSwain, Jason T. Huse, Bengt Westermark, Sven Nelander, Karin Forsberg-Nilsson, Lene Uhrbom, Naga Prathyusha Maturi, Patrick. J. Cimino, Eric C. Holland, Helmut Kettenmann, Cameron W. Brennan, Daniel J. Brat & Dolores Hambardzumyan (2019). Human Mesenchymal glioblastomas are characterized by an increased immune cell presence compared to Proneural and Classical tumors, OncoImmunology, 8:11, https://doi.org/10.1080/2162402X.2019.1655360.

Ioannis Kaffes, Frank Szulzewsky, Zhihong Chen, Cameron J. Herting, Ben Gabanic, José E. Velázquez Vega, Jennifer Shelton, Jeffrey M. Switchenko, James L. Ross, Leon F. McSwain, Jason T. Huse, Bengt Westermark, Sven Nelander, Karin Forsberg-Nilsson, Lene Uhrbom, Naga Prathyusha Maturi, Patrick. J. Cimino, Eric C. Holland, Helmut Kettenmann, Cameron W. Brennan, Daniel J. Brat & Dolores Hambardzumyan (2019). Human Mesenchymal glioblastomas are characterized by an increased immune cell presence compared to Proneural and Classical tumors, OncoImmunology, 8:11, https://doi.org/10.1080/2162402X.2019.1655360.

Ioannis Kaffes, Frank Szulzewsky, Zhihong Chen, Cameron J. Herting, Ben Gabanic, José E. Velázquez Vega, Jennifer Shelton, Jeffrey M. Switchenko, James L. Ross, Leon F. McSwain, Jason T. Huse, Bengt Westermark, Sven Nelander, Karin Forsberg-Nilsson, Lene Uhrbom, Naga Prathyusha Maturi, Patrick. J. Cimino, Eric C. Holland, Helmut Kettenmann, Cameron W. Brennan, Daniel J. Brat & Dolores Hambardzumyan (2019). Human Mesenchymal glioblastomas are characterized by an increased immune cell presence compared to Proneural and Classical tumors, OncoImmunology, 8:11, https://doi.org/10.1080/2162402X.2019.1655360.

Ioannis Kaffes, Frank Szulzewsky, Zhihong Chen, Cameron J. Herting, Ben Gabanic, José E. Velázquez Vega, Jennifer Shelton, Jeffrey M. Switchenko, James L. Ross, Leon F. McSwain, Jason T. Huse, Bengt Westermark, Sven Nelander, Karin Forsberg-Nilsson, Lene Uhrbom, Naga Prathyusha Maturi, Patrick. J. Cimino, Eric C. Holland, Helmut Kettenmann, Cameron W. Brennan, Daniel J. Brat & Dolores Hambardzumyan (2019). Human Mesenchymal glioblastomas are characterized by an increased immune cell presence compared to Proneural and Classical tumors, OncoImmunology, 8:11, https://doi.org/10.1080/2162402X.2019.1655360.

Ioannis Kaffes, Frank Szulzewsky, Zhihong Chen, Cameron J. Herting, Ben Gabanic, José E. Velázquez Vega, Jennifer Shelton, Jeffrey M. Switchenko, James L. Ross, Leon F. McSwain, Jason T. Huse, Bengt Westermark, Sven Nelander, Karin Forsberg-Nilsson, Lene Uhrbom, Naga Prathyusha Maturi, Patrick. J. Cimino, Eric C. Holland, Helmut Kettenmann, Cameron W. Brennan, Daniel J. Brat & Dolores Hambardzumyan (2019). Human Mesenchymal glioblastomas are characterized by an increased immune cell presence compared to Proneural and Classical tumors, OncoImmunology, 8:11, https://doi.org/10.1080/2162402X.2019.1655360.

Ioannis Kaffes, Frank Szulzewsky, Zhihong Chen, Cameron J. Herting, Ben Gabanic, José E. Velázquez Vega, Jennifer Shelton, Jeffrey M. Switchenko, James L. Ross, Leon F. McSwain, Jason T. Huse, Bengt Westermark, Sven Nelander, Karin Forsberg-Nilsson, Lene Uhrbom, Naga Prathyusha Maturi, Patrick. J. Cimino, Eric C. Holland, Helmut Kettenmann, Cameron W. Brennan, Daniel J. Brat & Dolores Hambardzumyan (2019). Human Mesenchymal glioblastomas are characterized by an increased immune cell presence compared to Proneural and Classical tumors, OncoImmunology, 8:11, https://doi.org/10.1080/2162402X.2019.1655360.

Ioannis Kaffes, Frank Szulzewsky, Zhihong Chen, Cameron J. Herting, Ben Gabanic, José E. Velázquez Vega, Jennifer Shelton, Jeffrey M. Switchenko, James L. Ross, Leon F. McSwain, Jason T. Huse, Bengt Westermark, Sven Nelander, Karin Forsberg-Nilsson, Lene Uhrbom, Naga Prathyusha Maturi, Patrick. J. Cimino, Eric C. Holland, Helmut Kettenmann, Cameron W. Brennan, Daniel J. Brat & Dolores Hambardzumyan (2019). Human Mesenchymal glioblastomas are characterized by an increased immune cell presence compared to Proneural and Classical tumors, OncoImmunology, 8:11, https://doi.org/10.1080/2162402X.2019.1655360.

My curriculum vitae does not appear in the electronic version of my paper for reasons of data protection.

My curriculum vitae does not appear in the electronic version of my paper for reasons of data protection.

List of Publications

1. **Kaffes I**, Szulzewsky F, Chen Z, Herting CJ, Gabanic B, Velázquez Vega JE, Shelton J, Switchenko JM, Ross JL, McSwain LF, Huse JT, Westermark B, Nelander S, Forsberg-Nilsson K, Uhrbom L, Maturi NP, Cimino PJ, Holland EC, Kettenmann H, Brennan CW, Brat DJ, Hambardzumyan D. Human Mesenchymal glioblastomas are characterized by an increased immune cell presence compared to Proneural and Classical tumors. *Oncoimmunology*. 2019;8(11):e1655360. (Impact Factor at the time of publication: 5.333)

2. Herting CJ, Chen Z, Pitter KL, Szulzewsky F, **Kaffes I**, Kaluzova M, Park JC, Cimino PJ, Brennan C, Wang B, Hambardzumyan D. Genetic driver mutations define the expression signature and microenvironmental composition of high-grade gliomas. *Glia*. 2017;65(12):1914-26. (Impact Factor at the time of publication: 6.200)

3. **Kaffes I**, Moser F, Pham M, Oetjen A, Fehling M. Global health education in Germany: an analysis of current capacity, needs and barriers. *BMC Medical Education*. 2016;16(1):304. (Impact Factor at the time of publication: 1.312)

Acknowledgments

I would like to thank my supervisor Prof. Helmut Kettenmann for his guidance, scientific advice, and especially for creating the opportunity for me to pursue a research experience in the United States.

Special thanks go to Prof. Dolores Hambardzumyan, who not only was gracious enough to accept me at her laboratory at Emory University, but who, through her intellectual curiosity, passion for science, and unwavering support, became a mentor and overall inspiration.

I also thank my fellow lab members and collaborators, who welcomed me with open arms and taught me the ways of scientific practice and progress.

Words cannot express my gratitude to my parents Ina and Christodoulos, my brother Maximilian, my girlfriend Raya, as well as my grandparents, who have always had my back and helped me maintain a healthy perspective on life.

My friends, who have provided scientific advice and shown incredible support, also deserve special thanks.

Finally, I would like to dedicate this work to my cousin Ioannis, a true fighter.